Frequency tuning of IR first-overtone CO laser radiation by diffraction grating and frequency selective output couplers

Final Report

Time period: August 1998 - January 1999

Scientific leader:
Prof. A. Napartovich

Dr. A. Kurnosov

Mr. N. Turkin

Principal Investigator,
Scientific Leader
Prof. A. Ionin

Mr. A. Kotkov

Mr. L. Seleznev

Mr. D. Sinitsyn

Mr. Yu. Klimachev

Moscow, 1999

19990203 039

AQF99-05-0836

Table of contents

REPORT DOCUMENTATION PAGE

Form Approved OMB No. 0704-0188

1. AGENCY USE ONLY (Leave blank)	2. REPORT DATE	3. REPORT TYPE AND DATES COVERED
	1999	Final Report

4. TITLE AND SUBTITLE

Frequency Tuning Of IR First Overtone CO Laser Radiation By Diffraction Grating And Frequency Selective Output Couplers

5. FUNDING NUMBERS

F61775-98-WE109

6. AUTHOR(S)

Dr. Andre Ionin

7. PERFORMING ORGANIZATION NAME(S) AND ADDRESS(ES)

P. N. Lebedev Physical Institute
53 Leninsky Prospect
Moscow 117924
Russia

8. PERFORMING ORGANIZATION REPORT NUMBER

N/A

9. SPONSORING/MONITORING AGENCY NAME(S) AND ADDRESS(ES)

EOARD
PSC 802 BOX 14
FPO 09499-0200

10. SPONSORING/MONITORING AGENCY REPORT NUMBER

SPC 98-4076

11. SUPPLEMENTARY NOTES

12a. DISTRIBUTION/AVAILABILITY STATEMENT

Approved for public release; distribution is unlimited.

12b. DISTRIBUTION CODE

A

13. ABSTRACT (Maximum 200 words)

This report results from a contract tasking P. N. Lebedev Physical Institute as follows: The contractor will investigate, both experimentally and theoretically, the feasibility of frequency tuning the first overtone carbon monoxide laser radiation by the use of diffraction gratings and frequency-selective output couplers.

14. SUBJECT TERMS

EOARD, CO lasers, Mid-IR lasers

15. NUMBER OF PAGES

39

16. PRICE CODE

N/A

17. SECURITY CLASSIFICATION OF REPORT	18. SECURITY CLASSIFICATION OF THIS PAGE	19. SECURITY CLASSIFICATION OF ABSTRACT	20. LIMITATION OF ABSTRACT
UNCLASSIFIED	UNCLASSIFIED	UNCLASSIFIED	UL

NSN 7540-01-280-5500

Standard Form 298 (Rev. 2-89)
Prescribed by ANSI Std. 239-18
298-102

1. Introduction

As was shown in [1-3], pulsed multiline first-overtone (FO) CO laser runs within the spectral range of 2.5-4.0 µm considerably extended as compared to pulsed FO CO laser spectrum previously observed in [4-9] and comparable with the spectral range of tunability for single line low-pressure cw FO CO laser [10,11]. Output efficiency up to 5% was obtained for FO CO laser running within relatively narrow spectral range of 2.5-2.7 µm determined by spectral characteristics of output couplers [1-3]. It was pointed out in [1-3] that, taking into account useless optical losses for multilayer dielectric output couplers, total FO CO laser efficiency reaches 6.0-6.5% for the laser with such a narrow spectrum. Obviously, an extension of FO CO laser spectrum and a decrease of the useless intracavity optical losses introduced by laser mirrors has to result in considerable increase of the output efficiency. A potential feasibility of such an increase of FO CO laser efficiency up to 15-20% was indicated in [7-9].

Various combinations of dielectric output couplers with low optical losses produced in the USA were used for obtaining lasing within broad band spectral region. An achievement of FO CO laser efficiency up to 11% is reported in the given scientific report. A comparison of experimental and theoretical results does indicate a feasibility of further increase of FO CO laser efficiency up to 20%. Tunable single vibrational-rotational line lasing for pulsed FO CO laser within spectral range of ~2.74-4.15 µm was experimentally demonstrated.

2. Multiline Pulsed FO CO Laser with Output Efficiency 11%

2.1 Experimental conditions

The experiments were carried out on cryogenically cooled e-beam controlled discharge laser setup with active length of 1.2 m and active volume of 0.85 l. The active volume was limited by diameter of output couplers. Pump pulse length was 25 µs. Laser mixture $CO:N_2:He=1:9:10$ at gas density 0.12 Amagat and initial gas temperature 100 K was used. The measuring procedure was the same as in [1-3,7-9]. Home-made spectrometer was used for spectral measurements. Its description is presented in **Appendix I**.

Special attention was given to dielectric output couplers, that were produced by Rocky Mountain Instrument Co., USA. Three sets of the output couplers (two laser mirrors in one set) were used for the laser resonator. Although the order was to have laser mirrors with high reflectivity (92, 97 and 99.9%) within spectral range of 2.4-4.2 µm and low reflectivity lesser than 10% for that of 4.6-6.0 µm, bearing in mind fundamental band (FB) lasing suppression [7-9], spectral characteristics of the laser mirrors did not correspond to our wish. However, as compared to the mirrors used in [1-3],

the new mirrors had lower useless optical losses. One can see in Fig. 1 an effective reflectivity $R=(R_iR_j)^{1/2}$ ($i, j=1, 2$) for the mirror of the equivalent symmetric laser resonator. As compared to mirrors used in [1-3], the spectral range for the high reflectivity of the new ones was extended to the long wavelengths region. The mirrors M98 and M99 had a radius of curvature of 15 m and 10 m, respectively, whereas the mirror M92 was a flat one. The reflectivity of the mirrors was noticeably irregular within ~2.5-3.0 μm spectral range (Fig.2.1). A thorough measurements of transmittance and reflectance of the mirrors were done, the results being presented in **Appendix II**.

2.2 Experimental results

Such a behavior of the reflectivity led to a suppression of FO lasing within spectral intervals corresponding to the low reflectivity (Fig.2.1a-c), i.e. FO CO laser spectrum correlated with the spectral characteristics of the laser mirrors. Very weak laser line, corresponding to 37→35 vibrational transition with longer wavelength of 4.1 μm, than we had before, was observed when M92+M92 set of the mirrors was used (Fig. 2.1a). However, the output energy of the laser with this set of the mirrors was rather low, because the effective reflectivity for the laser resonator was lower and, besides, the laser resonator consisted of two flat mirrors instead of combination of concave and flat mirror. FO CO laser ran on vibrational transitions from 15→13 up to 37→35 (wave length (λ) range was from 2.83 up to 4.09 μm) except transitions from 19→17 up to 20→18 (λ=2.98 - 3.07 μm) for mirror combination M92+M92; from 14→12 up to 35→33 (λ=2.80 - 3.93 μm) except vibrational transition 19→17 (λ=2.98 - 3.02 μm) for mirror combination M92+M99 and on vibrational transitions from 19→17 up to 34→32 (λ=3.00 - 3.83 μm) for mirror set M98+M98. For all the sets of the mirrors FB lasing also took place (Fig.2.1) despite the low reflectivity (especially for M92+M92 and M92+M99 sets) of the mirrors for the FB spectral range. Pulse length for FO CO laser was 1.5-6 ms and for FB CO laser 0.6-1.5 ms (on 0.1 level) depending on other conditions.

The dependencies of specific output energy (SOE) on specific input energy (SIE) delivered into the electric discharge for the CO laser with these two sets of the mirrors M92+M99 and M98+M98 are presented in Fig. 2.2 both for FO and FB spectral ranges. Total output energy extracted from both sides of the laser was measured The SOE ~25 J/l Amagat for the FO CO laser was obtained at SIE ~280 J/l Amagat, when using M98+M98 set. For the same set, FB CO laser SOE reached ~20 J/l Amagat. Output efficiency came up to 11% for FO CO laser (Fig. 2.3) going over the output efficiency of the laser with M92+M99 set, FB CO laser efficiency reaching up to 9%. The SIE rise up to ~700 J/l Amagat (M92+M99 mirror set) resulted in SOE ~50 J/l Amagat, output efficiency

being~8% (Fig. 2.2b). In case of M98+M98 mirror set we limited SIE because of a danger of multilayer laser mirrors damage due to high total (FO+FB) energy density on the laser mirrors.
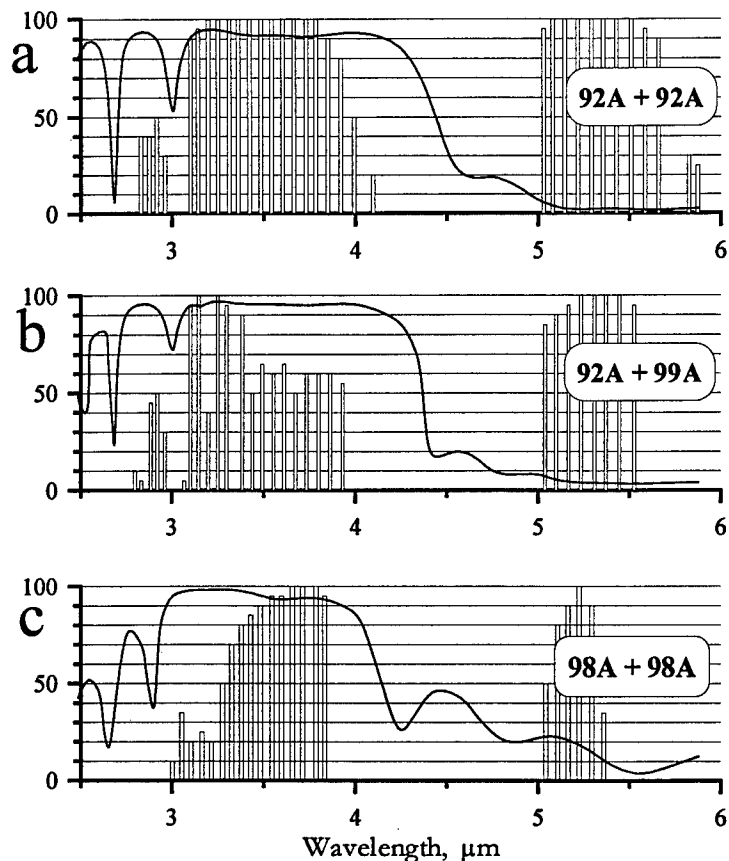

Fig.2.1. Effective reflectivity of output couplers and experimental output laser spectra for different mirror sets
CO:N_2:He=1:9:10; N=0.12 Amagat; SIE=300 J/l Amagat; T=100 K
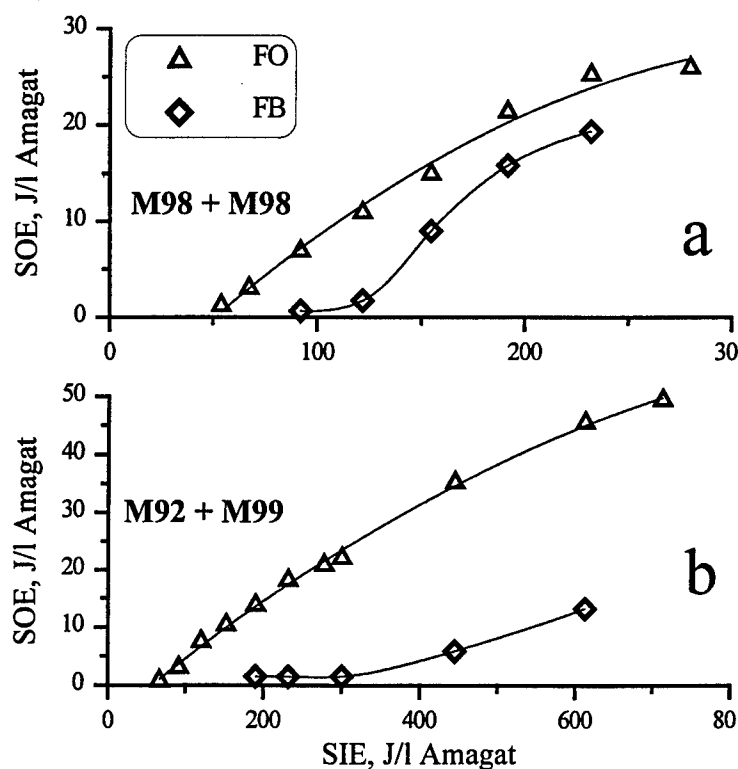
Fig.2.2. Specific output energy (SOE) of first overtone (FO) and fundamental band (FB) CO laser vs. specific input energy (SIE) for two different output couplers
CO:N_2:He=1:9:10; N=0.12 Amagat; T=100 K
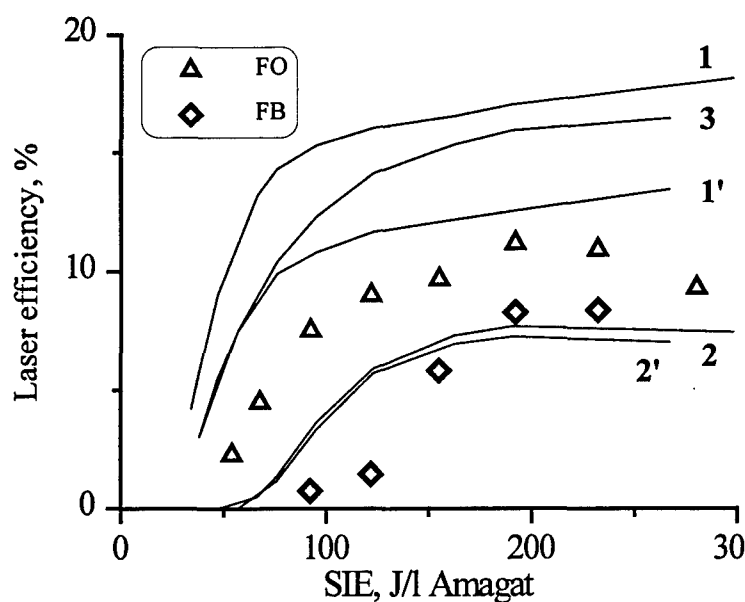
Theoretical results: 1, 1', 3 - first-overtone (FO) lasing; 2, 2' - fundamental band (FB) lasing

1, 2 - base model;
1', 2' - additional nonselective optical losses are included (0.5% per single pass);
3 - FB lasing is assumed to be suppressed, additional optical losses are the same

$CO:N_2:He=1:9:10$;   N=0.12 Amagat;
SIE=300 J/l Amagat; T=100 K

Fig.2.3. Laser efficiency vs. specific input energy (SIE) (experiment -points; theory - curves)

It should be noted that FO CO lasing was observed within initial gas temperature interval 100-220 K, only threshold lasing being observed at 220 K and SIE ~700 J/l Amagat (M99+M99 mirror set).

2.3. Theoretical results

Theoretical modeling of the FO CO laser for conditions corresponding to the experiments was performed for the combinations of the mirrors M98+M98 and M92+M99. Experimentally measured cavity parameters (see **Appendix II**) were included in the model which coincide essentially with the published earlier model [1-3,7-9]. The only difference was that at present in our model the laser transitions in the fundamental band were included, too. Therefore, it was possible to simulate simultaneous lasing in both bands (first-overtone and fundamental).

High values of the reflection coefficient for the mirrors made laser characteristics more sensitive to an exact magnitude of an additional intracavity optical loss not included in the model, i. e. diffraction loss and optical loss depending on gas refractive index gradients. In Fig. 2.3 calculated laser efficiency for FO (curve 1) and FB (curve 2) lasing is compared with the experimental data for the mirror set M98+M98. The FO laser efficiency predicted is about 1.5 times higher than one measured in the experiments, while the efficiency for the FB lasing is described more or less satisfactorily. To evaluate sensitivity of calculations to the exact value of the intracavity loss additional optical losses were introduced equal to 0.5% per single pass. The result of theoretical predictions is shown in Fig. 2.3 (curve 1' for the FO and curve 2' for the FB efficiency, respectively). It can be seen that the FO curve came closer to experimental points while the FB efficiency is

insensitive to the variation of optical losses. Calculations of the FO laser efficiency in an assumption that FB lasing is totally suppressed for the same cavity gave the curve 3 in Fig. 2.3. It means that additional absorption of radiation in the fundamental band can lead to the further increase of the FO laser efficiency up to 15-17% for the given set of the mirrors. Application of optimal laser mirrors (no spectral holes within 2.5-3.0 μm regions) will increase output efficiency up to 20%, which confirms the results of [1-3].
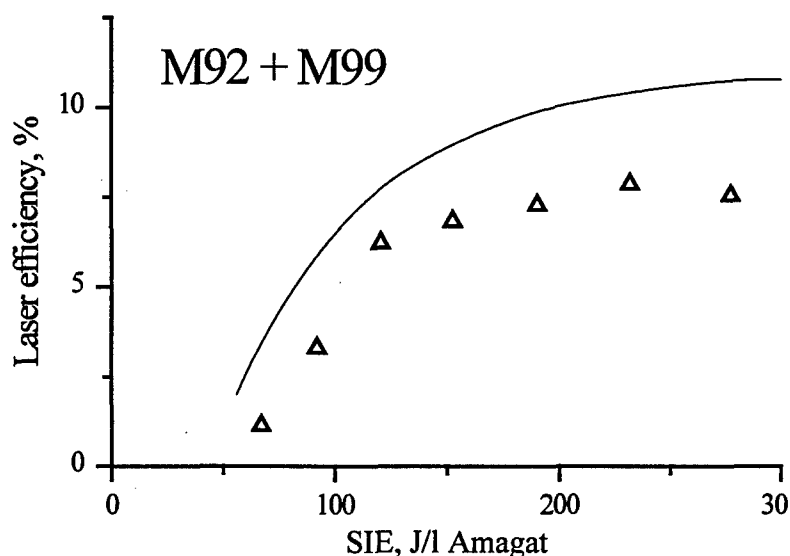
Fig.2.4. Laser efficiency vs. specific input energy (SIE) (experiment - points; theory - curves)

CO:N₂:He=1:9:10;
N=0.12 Amagat; T=100 K

Similar calculations were made for the laser efficiency with the cavity using mirrors M92+M99 (see Fig. 2.4). Theoretical predictions are higher for the FO lasing and no any FB lasing was found numerically. FB lasing is close to the threshold resulting in higher sensitivity of calculations to the details of the model. Therefore this discrepancy may be neglected.
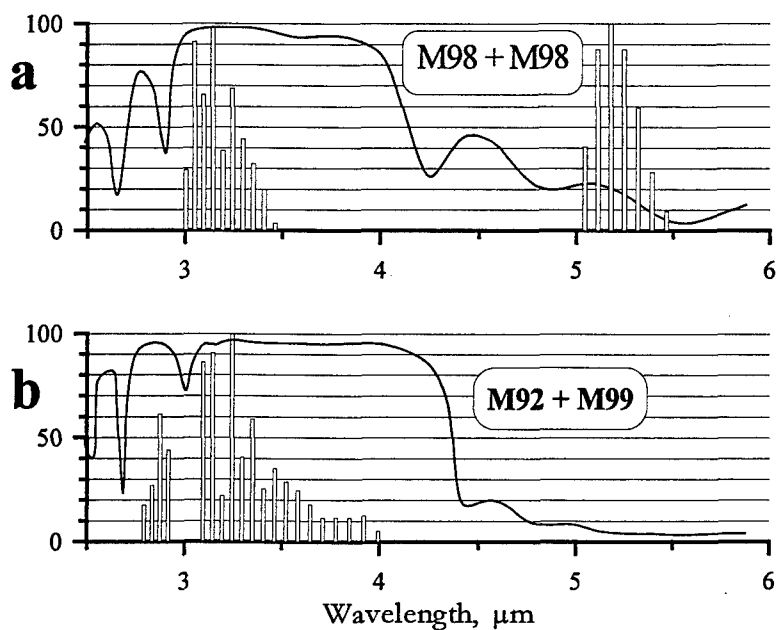
Fig.2.5. Theoretical output laser spectra and effective reflectivity of output couplers for two mirror sets

In Fig. 2.5a the computed laser spectrum is shown for the cavity with mirrors M98+M98 and with additional losses 0.5% per single pass. Comparing it with the experimental one presented in Fig.1c, the conclusion can be made that a good correlation between the FB spectra takes place, while the agreement for the FO spectra is not so good. The calculated FO laser spectrum is narrower and concentrated at the short wavelength part. Calculated laser energy is much higher for this part of spectrum as compared to the experimental results. The discrepancy in spectra was supposed to be connected with high reflectivity of the output coupler and, hence, its low transmittance. The mirror transmittance reflectance and optical loss for this part of spectrum, calculated by using data of Appendix II are presented in Fig. 2.6, in which one can see that if intracavity optical loss is up to 1.5%, its value is comparable with transmittance and, therefore, in this part of spectrum loss of energy is comparable with output energy. We analyzed numerically the influence of such an optical loss upon FO CO laser spectrum for FO CO laser with M98+M98 set of mirrors. The results of calculations are presented in Fig. 2.7. It was assumed, that additional intracavity losses are not spectrally selective and are 0.5%, 1.0% and 1.5% per single pass, respectively. Looking at Fig. 2.7 one can conclude that the laser spectrum deformation induced by the optical losses growth is much lower than one observed in the experiments.
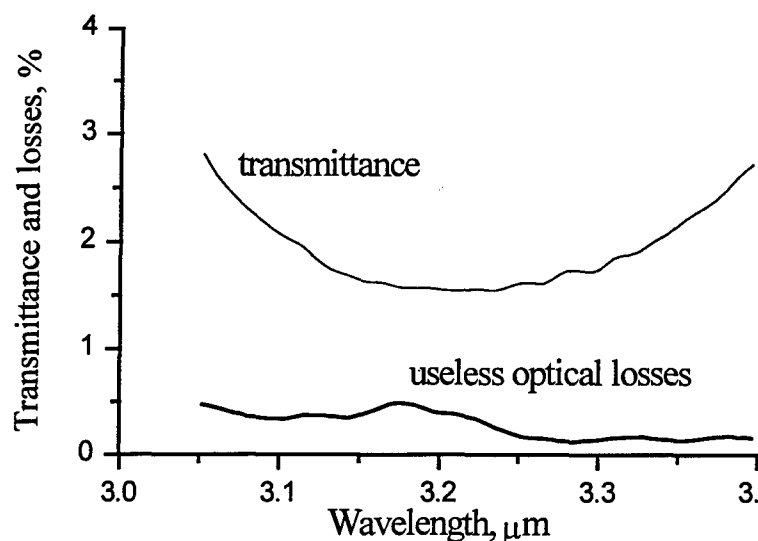
Fig.2.6. Spectral transmittance and useless optical losses for mirror M98

It should be noted that calculated FO laser efficiency for additional losses 1% and 1.5% per single pass is lower than measured experimentally. In particular, for the SIE 190 J/l Amagat calculated FO CO laser efficiency is 9.5% and 7.25%, respectively, and lesser than experimentally measured one (10%). This result demonstrates that optical quality of the active medium in our experiments is high enough. It means that further progress in characteristics of optical elements in the cavity will surely result in increase of the FO CO laser efficiency.

The disagreement between calculated and measured FO CO laser spectra can be considered as a strong indication that our kinetic model is not quite adequate to the real dynamics of the vibration distribution function. The observed discrepancy can be interpreted as follows: the dependence of the vibration exchange (V-V) probability for the high vibrational levels differs from traditionally accepted formulas. It means that the existing approximations for V-V exchange rate coefficients should be critically examined once more and new approaches should be applied including effects of multiquantum exchange effects [13,14].
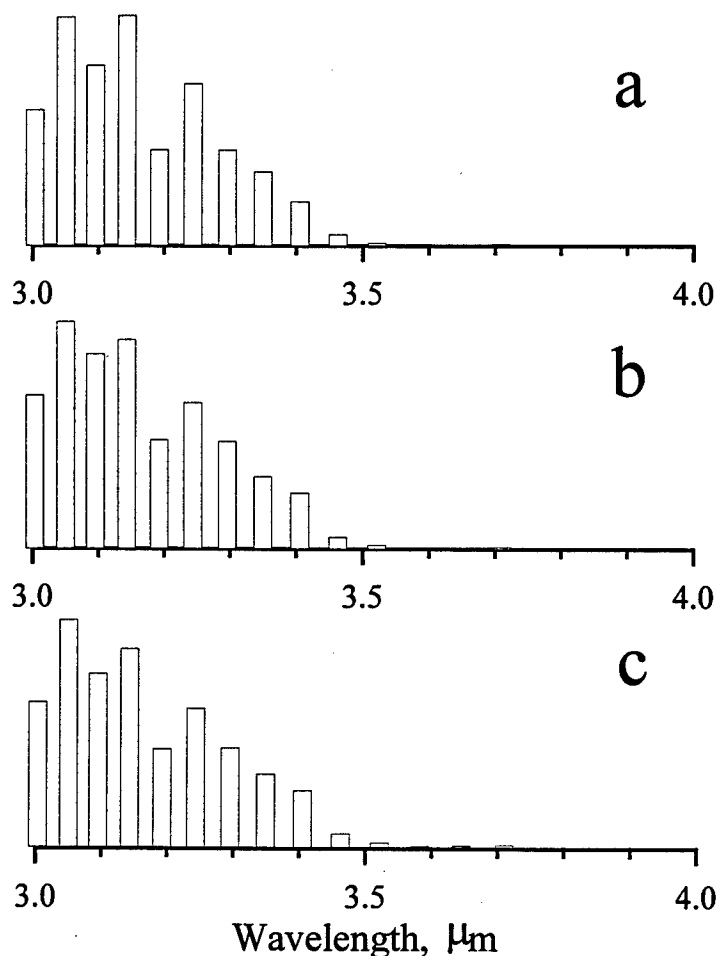
Fig.2.7. Output laser spectra calculated for different additional optical losses per single pass 0.5% (a); 1.0% (b); 1.5% (c.).

SIE=190 J/l Amagat

Wavelength, μm

The calculated spectrum of the FO CO laser with mirror set M92+M99 presented in Fig. 2.5b also contains lower energy corresponding to high vibrational transitions in comparison with the experiment. However, the discrepancy between theory and experiment in this case is not so strong.

2.4 Conclusions

Using dielectric mirrors with high reflectivity within extended spectral range and with lower optical losses enabled us to double pulsed FO CO laser efficiency, as compared to one obtained in [1-3], the output efficiency coming up to 11%. Specific output energy came up to ~50 J/l Amagat. FO

CO lasing was observed within initial gas temperature interval 100-220 K. The long wavelength region was extended up to 4.1 μm. Bearing in mind previous results [1-3], one can conclude, that multiline pulsed FO CO lasing range lies within 2.5-4.1 μm. The results of the theoretical calculations of the laser efficiency are in a good agreement with the experimental ones. Being based on these results the theory predicts, that FO CO laser efficiency can be as high as 20%. However, discrepancies observed in comparison of predicted and measured laser spectra indicate the necessity of modifying the kinetic description of vibrational kinetics.

3. Tunable single line pulsed FO CO laser

3.1. Experimental conditions

The FO CO laser resonator consisted of a diffraction grating operating in Littrow configuration and concave (r=10 m) copper mirror, the former being located at a distance of 0.4 m from Brewster window made of CaF_2 and the latter being installed at the laser chamber. Polarization plane of intracavity radiation was perpendicular to grating grooves (S-polarization). The laser resonator length was 2.5 m. There were two diaphragms inside the laser resonator with diameter 50 mm near the copper mirror and ~30 mm near the grating. The optical volume was 0.85 l. FO CO laser radiation was extracted through the zero diffraction order of the grating.

Two different diffraction gratings (G) made in Russia were used for spectral selection and tuning of FO CO laser radiation. Maximum efficiency for the first diffraction order took place at wavelength λ_{max} =3.0 μm (G1) and 3.2 μm (G2) at normal incidence of nonpolarized laser radiation for these two gratings according to their certificates. Both gratings were made of Al coated glass and had 200 grooves per mm.

Thin (~4 mm) plane parallel CaF_2 plate placed inside the laser resonator under the Brewster angle to the optical axis was used for adjustment of the resonator. When comparing the angular divergence of the laser determined by geometric factors (resonator length, radius of curvature of copper mirror and diameter of the intracavity diaphragm) and angular dispersion of the grating, one could conclude, that lasing might take place within the spectral interval of ~15 cm^{-1}. The laser spectra observed in the experiment did consist of one strong (central) and two very weak (adjacent) vibrational-rotational lines 4 cm^{-1} apart. We called this regime single line lasing because the energy of the adjacent lines was an order of magnitude lesser than the energy of the central line. The laser spectra consisted of two strong adjacent lines were also observed. The real single line regime of FO CO laser operation was observed, when diaphragm diameter was decreased down to 15 mm.

Wavelength tuning of the laser radiation was effected by rotation of the grating. The rotation angle of the grating was controlled by using auxiliary visible laser beam reflected from the mirror

fixed at the grating and observed on a scale located at the distance of 4 m from the grating. FO CO laser spectrum was detected by long focus spectrometer (**Appendix I**).

Laser mixture $CO:N_2:He=1:9:10$ at initial gas temperature ~100 K and gas density 0.12 Amagat was used.

3.2. Experimental results

At the first experiments FO CO laser radiation was tuned within single 22→20 vibrational band over the vibrational-rotational lines from J=6 up to J=17 (**Fig. 3.1**). The grating G1 was used. From the figure one can see the laser to be tuned partly over several vibrational-rotational lines belonged to the vibrational band 23→21. The laser was tuned within 3.11-3.17 µm wavelength interval. Some irregularity of spectral distribution for 22→20 vibrational band, which can be connected with intracavity absorption by atmospheric air, was observed. **Fig. 3.2** demonstrates the dependencies of SOE and single line FO CO laser efficiency on SIE for the laser wavelength ~3.13 µm corresponding to the vibrational-rotational line P(10). Threshold lasing took place at SIE of ~100 J/l Amagat. The maximum SOE of ~50 mJ/l Amagat was observed at SIE of 260 J/l Amagat, output efficiency being extremely poor ~0.02%. Further research demonstrated, that for above experiments we did not choose the optimal wavelength region for given diffraction gratings.

Much more SOE and higher output efficiency for single line FO CO laser was observed for longer laser wavelengths and higher vibrational transitions, which was connected with spectral characteristics of the diffraction gratings. The dependencies of SOE and threshold SIE upon laser wavelength within 35→33 vibrational band are presented in **Fig. 3.3**. One can see that the SOE for the center of the band (vibrational-rotational lines P(11), P(12)) is higher than 0.3 J/l Amagat, i.e. six times higher as compared to vibrational band 22→20 (**Fig. 3.1**). Output efficiency reached 0.1% for 33P(11) and 33P(12) lines (we used short notation for vibrational-rotational transition V+2→V; J-1→J as V P(J)).
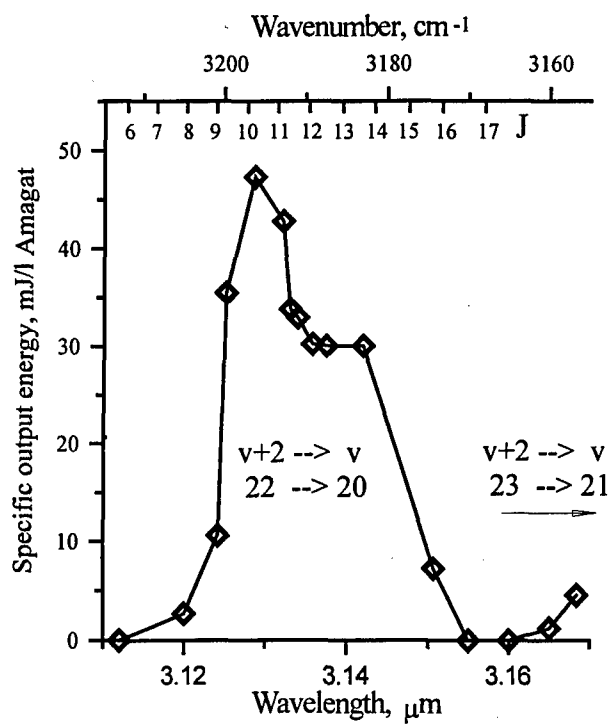
Fig.3.1. Specific output energy (SOE) vs. wavelength for vibrational transitions 22→20 and 23→21.

CO:N_2:He=1:9:10;
SIE=290 J/l Amagat; T=100 K
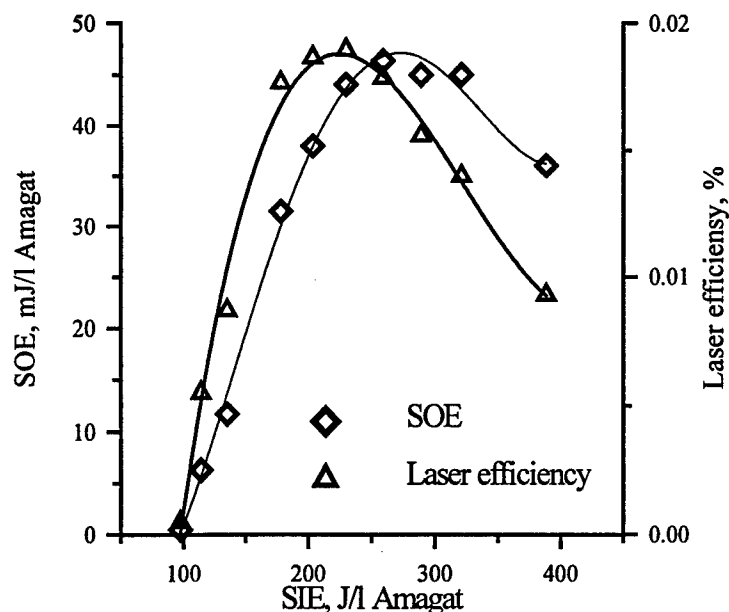
Fig.3.2. Specific output energy (SOE) and single line FO CO laser efficiency vs. specific input energy (SIE) for vibrational-rotational line 22→20 P(10).
CO:N_2:He=1:9:10; T=100 K

The dependence of threshold SIE on laser wavelength was asymmetric. When tuning laser wavelength to longer ones, e.g. from 3.92 μm up to 3.94 μm, the threshold SIE increased two fold. However, when tuning the wavelength to shorter ones (P(J) changed from P(14) down to P(8)), quite different situation was observed: threshold SIE was unchanged, being 100-120 J/l Amagat. The same behavior was also observed for other vibrational bands. One can see also in **Fig. 3.3** how single line FO CO laser was tuned from 35→33 vibrational band down to adjacent 34→32 band, which was accompanied by threshold SIE rise. Simultaneous lasing on adjacent vibrational transitions and different rotational lines with wavelength difference lying within spectral resolution of the laser optical scheme was experimentally observed.
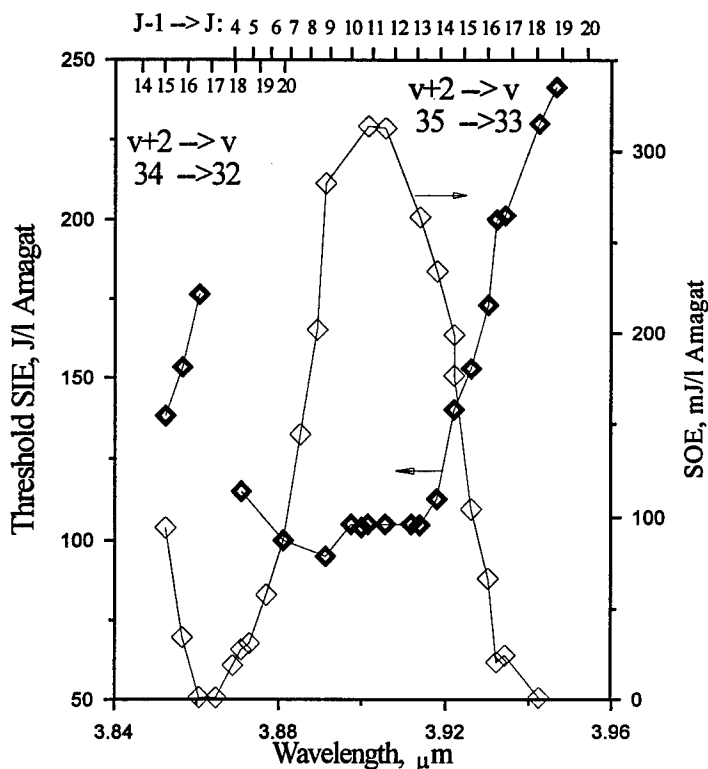
Fig.3.3. Specific output energy (SOE) and threshold specific input energy (SIE) vs. wavelength for vibrational transitions 35→33 and 34→32

CO:N_2:He=1:9:10; N=0.12 Amagat; SIE=230 J/l Amagat; T=100 K

Fig. 3.4(a,b) demonstrates SOE vs. SIE for different P(J) (J=15 and 7) for 35→33 vibrational band. For 33P(15) line threshold lasing took place at SIE 220 J/l Amagat, whereas for 33P(7) line at 130 J/l Amagat, as one can also see from **Fig. 3.3**. The dependencies in **Fig. 3.4(a,b)** are monotonous. **Fig. 4c** demonstrates the same dependence for the wavelength, where two FO CO laser rotational lines might operate corresponding to adjacent vibrational bands within the spectral resolution of the laser optical scheme: namely 33P(4) and 32P(17). As SIE increased, firstly FO CO lasing starts at low SIE ~120J/l Amagat, which is typical for laser transitions with lower J. Typical monotonous dependence SOE on SIE (compare **Fig. 3.4b** and **c**) is observed up to SIE 250 J/l Amagat. At this point its abrupt growth is observed. We consider the phenomenon as appearance of lasing on 32P(17) line with threshold SIE ~250 J/l Amagat. The same analysis of dependence SOE upon SIE for different wavelengths was also used for estimation of threshold SOE at simultaneous lasing on different rotational lines belonged to adjacent vibrational bands. It should be noted that above effect was not observed for adjacent 35→33 and 36→34 vibrational bands, as lasing on 36→34 band took place with lower SIE and within more narrow interval of rotational lines J, as compared to 35→33 band.
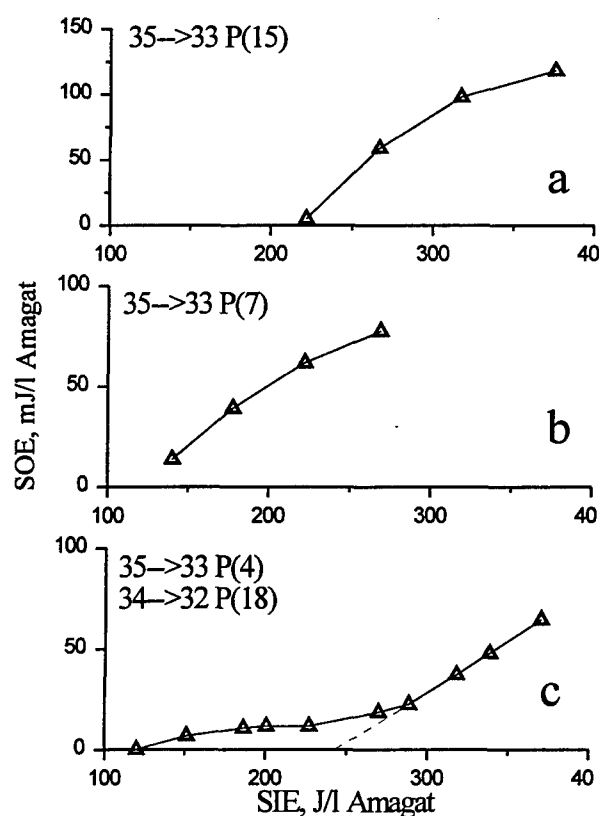
Fig.3.4. Specific output energy (SOE) vs. specific input energy (SIE) for different vibrational-rotational transitions

CO:N$_2$:He=1:9:10; N=0.12 Amagat; T=100 K

The grating G1 was successfully used for FO CO laser radiation tuning from 3.4 up to 4.1 μm (**Fig. 3.5**). The figure demonstrates SOE vs. laser wavelength. Solid lines represent the dependence, as laser was tuned over different rotational lines within single vibrational band. Dashed line goes through the maximum value of SOE for each vibrational band. Maximum SOE ~0.6 J/l Amagat was

obtained for 32→30 and 33→31 vibrational bands. For a long wavelength region, i.e. for higher vibrational transitions, maximum SOE decreased approximately linearly with vibrational number rise, the highest transition being 37→35. A decrease of SOE for shorter wavelengths was due to spectral properties of the grating G1.
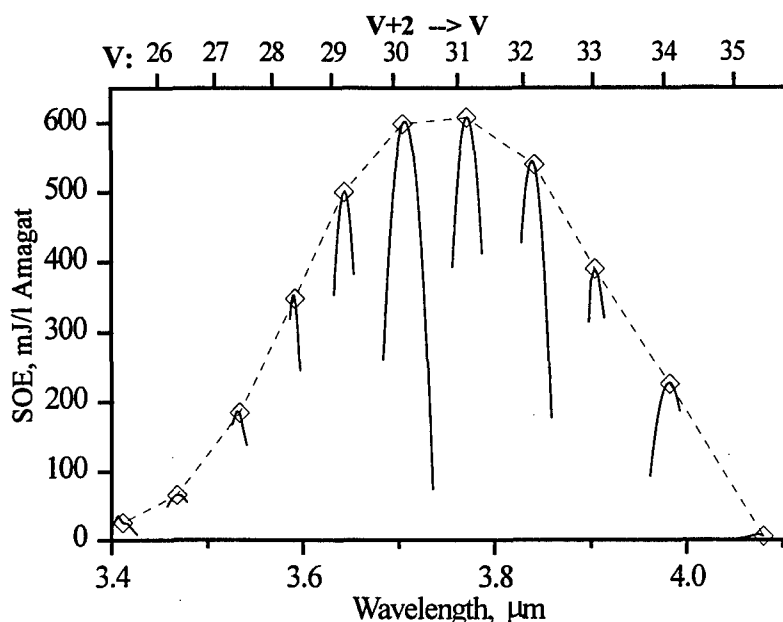
Fig.3.5. Specific output energy (SOE) vs. wavelength

CO:N$_2$:He=1:9:10; N=0.12 Amagat; SIE=230 J/l Amagat; T=100 K
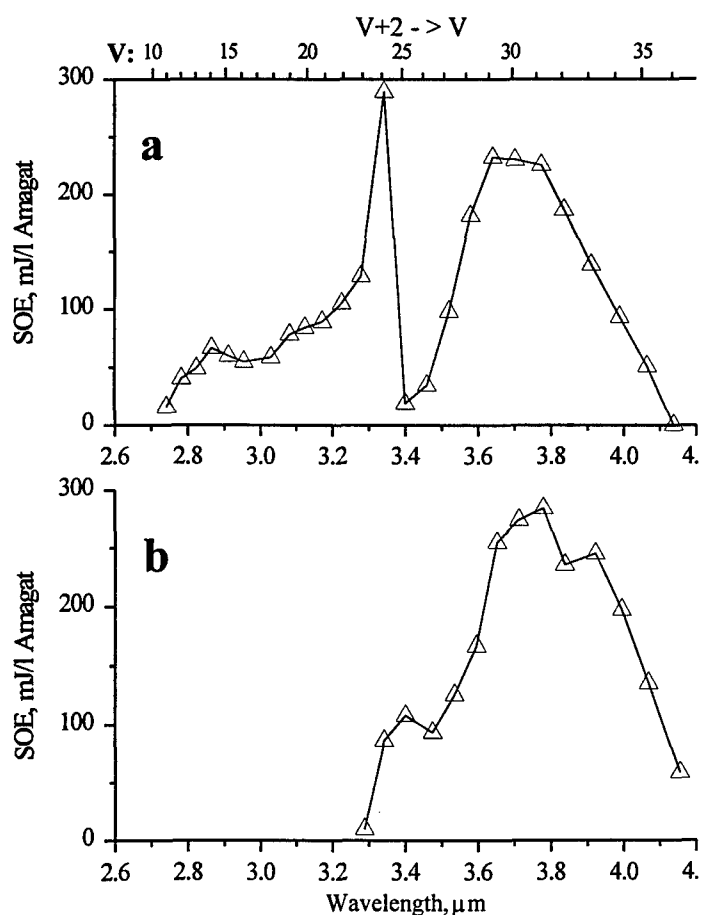
Fig.3.6. Specific output energy (SOE) vs. wavelength for two different diffraction grating G1 (**a**) and G2 (**b**).

CO:He=1:4; N=0.12 Amagat; SIE=230 J/l Amagat; T=100 K

Fig. 3.6 demonstrates SOE vs. laser wavelength for two different diffraction gratings G1 and G2 within wavelength range from 2.7 up to ~4.2 μm. Laser mixture CO:He=1:4 at gas density

0.12 Amagat was used. One can see that the spectral properties of the FO CO laser strongly depend on spectral characteristics of the diffraction grating used as an output coupler in Littrow configuration for S-polarized radiation (polarization plane of radiation was perpendicular to grating grooves). **Fig. 3.6a** demonstrates data obtained for the grating G1 used for the above experiments. The right part of the figure just corresponds to the **Fig. 3.5** and reflects the spectral properties of the grating G1 in long wavelength region. An anomaly (the spectral hole) in the dependence near the wavelength 3.3-3.4 μm is connected with redistribution of energy of radiation diffracted by the grating over diffraction orders with grating rotation. In particular, when $\lambda/d < 2/3$, where λ is radiation wavelength and d is spacing of a grating, radiation energy (intensity) is distributed over spectral orders m=-1, 0, +1 and +2 instead of m=0, +1 [15]. For the gratings used in the experiment (d=5 μm) the anomalies can arise at λ<3.33 μm. A decrease of SOE for grating G1 and lasing absence for grating G2 (λ_{max} =3.2 μm) at wavelength shorter than 3.3 μm is connected with spectral properties of the gratings and perhaps, partially with intracavity absorption of laser radiation by atmospheric air. The longest wavelength obtained by using the grating G2 was 4.15 μm, that corresponded to 38→36 vibrational transition.

3.3. Theoretical results

3.3.1. In our previous report [1] it was shown that using of spectral selective cavities with a spectral interval allowing for lasing of three or five overtone lines corresponding to neighboring vibration bands seems to be promising for achieving high efficiency comparable with free-running efficiency with suppressed fundamental band lasing. Requirements to output coupler or spectral filter manufacturing with necessary properties are much simpler for the narrow bands. Therefore, we continue our studies on methods of spectral selection in more detail.

To make conditions for our studies more realistic and definite, parameters of experimentally realized multilayer output couplers described in our previous report were taken as a basis. Namely, we took the maximum reflection coefficient of the mirror designated in [1] as M2 97.5% for the reflection in the allowed spectral range for the output coupler under consideration. Of total losses 2.5% the transmitted fraction was taken equal to 1.5% and 1% was assumed to be losses on absorption and scattering in the multilayer output coupler. It should be emphasized that all these figures were measured experimentally for the mirror M2 in the spectral range 3622-3836 cm^{-1}. Probably, the balance between transmission

and absorption/scattering losses in the mirror can be improved in a future. Other conditions: gas density 0.12 Amagat, temperature 100 K and composition $CO:N_2:He = 1:9:10$, specific input energy 220 J/l Amagat and discharge parameters (pulse duration 25 µs, initial value of the parameter E/N) were taken the same as in [1].

Our studies were focused on calculations of the FO CO laser efficiency for separate spectral components within the allowed spectral interval (ASI) and for total laser energy as functions of the central transition in the ASI. The mirror reflectance was assumed to be constant for five vibration transitions: $v_c - 2 \rightarrow v_c - 4$; $v_c - 1 \rightarrow v_c - 3$; $v_c \rightarrow v_c - 2$; $v_c + 1 \rightarrow v_c - 1$; $v_c + 2 \rightarrow v_c$. Here v_c is the number of the upper vibrational level for the central laser transition. Rotational quantum numbers were found automatically by simulation of competition process between rotational transitions during the laser pulse.
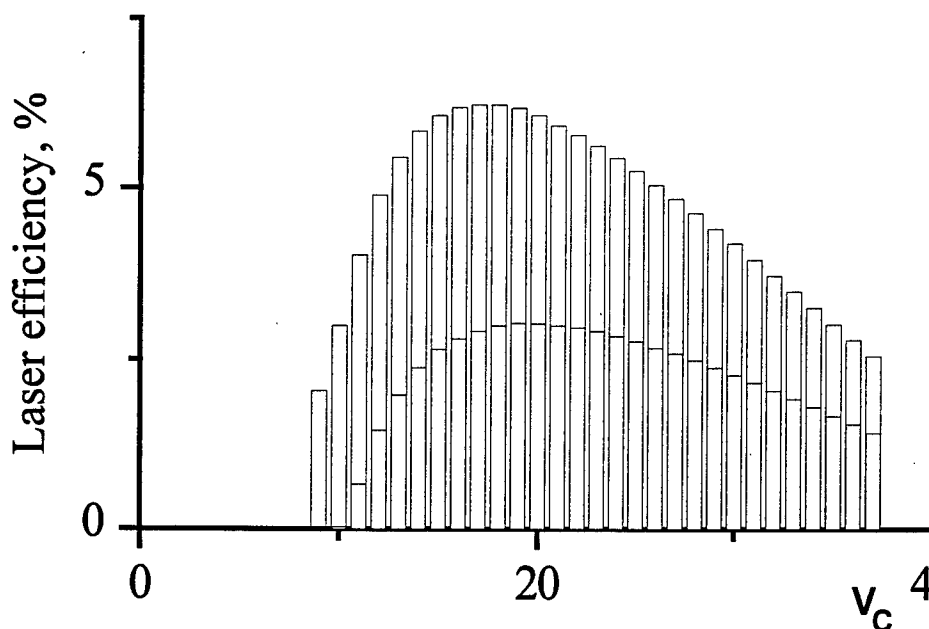
Fig.3.7 Calculated dependence of total output efficiency for five vibrational transitions ($V_c-2 \rightarrow V_c-4$; $V_c-1 \rightarrow V_c-3$; $V_c \rightarrow V_c-2$; $V_c+1 \rightarrow V_c-1$; $V_c+2 \rightarrow V_c$) and output efficiency for the lowest transition ($V_c-2 \rightarrow V_c-4$) for FO CO laser with narrow-band selective resonator upon quantum number of central vibrational transition V_c. Specific input energy is 220 J/l Amagat. The diagram corresponding to the laser efficiency on the lowest transition is shaded.

Results of numerical calculations displayed in **Fig. 3.7** demonstrate that the maximum laser efficiency for described conditions is above 6% in contrast to 3% computed in [1] for similar conditions except cavity threshold gain. Our model

predicts quite uneven distribution of laser energy over the selected five lines. In particular, for $v_c > 20$ the lowest transition (with shortest wavelength) inputs more than 50% of the total energy, i.e. the output efficiency for the single vibrational band can exceed 3%. This fact opens a new way for increase the single line efficiency for the FO CO laser, in particular for high vibrational transitions. It might be preferable to employ the selective laser cavity with the ASI including 5 vibrational bands, and then select the lowest transition from the total output pulse, i.e. extracavity single line selection can be preferable. It was shown earlier that the maximum laser efficiency in the overtone band is achieved in the limit of spectral selective cavity having a high reflectance in a very broad spectral range from about 2.5 μm to 4.0 μm and very low reflectance (less than 1%) for radiation in the fundamental band. These are very severe conditions for manufacturing such output couplers. Therefore it is very important that there exists an alternative way to realize a high efficiency for the overtone band: it is necessary to manufacture the output coupler with low losses and high reflectance (on the order of 97-98%) in the comparatively narrow spectral interval. Having no special requirements to the exact position of the ASI, the center of it should correspond to transitions from the level numbers 15-25.
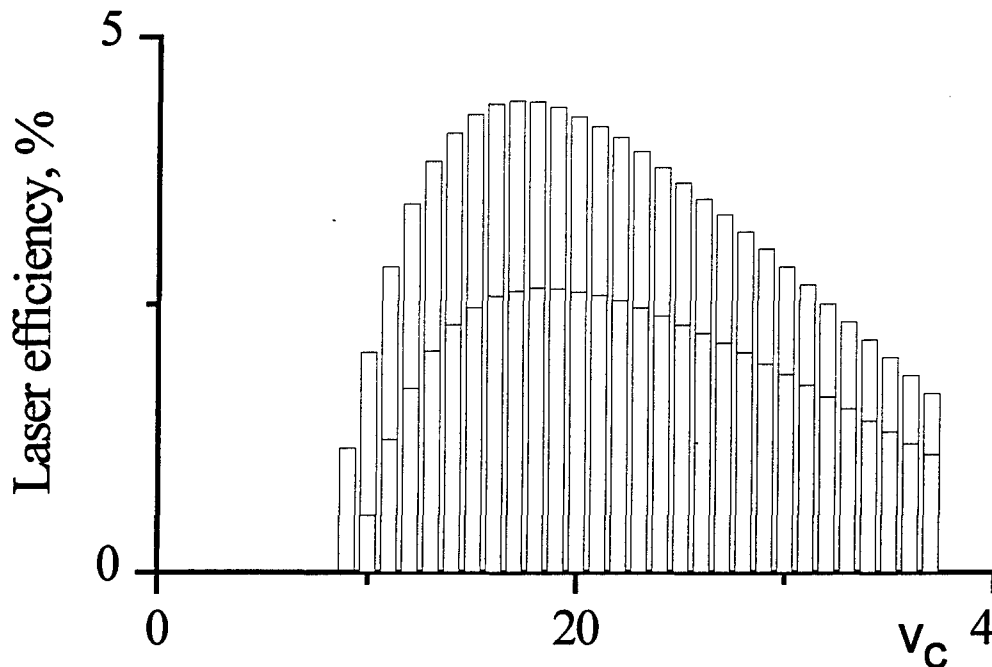
Fig.3.8. Calculated dependence of total output efficiency for three vibrational transitions (V_c-1→V_c-3; V_c→V_c-2; V_c+1→V_c-1) and output efficiency for the lowest transition (V_c-1→V_c-3) for FO CO laser with narrow-band selective resonator **upon** quantum number of central vibrational transition V_c. Specific

input energy is 220 J/l Amagat. The diagram corresponding to the laser efficiency on the lowest transition is shaded.

Similar studies were performed for spectral selective output couplers allowing for lasing of 3 transitions: $v_c - 1 \rightarrow v_c -3$; $v_c \rightarrow v_c -2$; $v_c + 1 \rightarrow v_c -1$. **Fig. 3.8** demonstrates that the total efficiency can be higher than 4%, while the efficiency for the lowest transition can be higher than 2.5%. These are very promising figures for realization of the high efficient FO CO laser with a comparatively narrow spectrum.

Concluding, the FO CO laser efficiency for the selective high-quality cavity can achieve more than 6% when the ASI includes 5 neighboring vibration transitions and more than 4% when 3 vibration transitions are lasing. For positions of the ASI center corresponding to transitions from 15th-25th levels more than a half of laser energy is contained in radiation on the single vibrational transition. These results were calculated for the output coupler losses in which were 40%. Further improving of the output coupler will increase the available laser efficiencies.
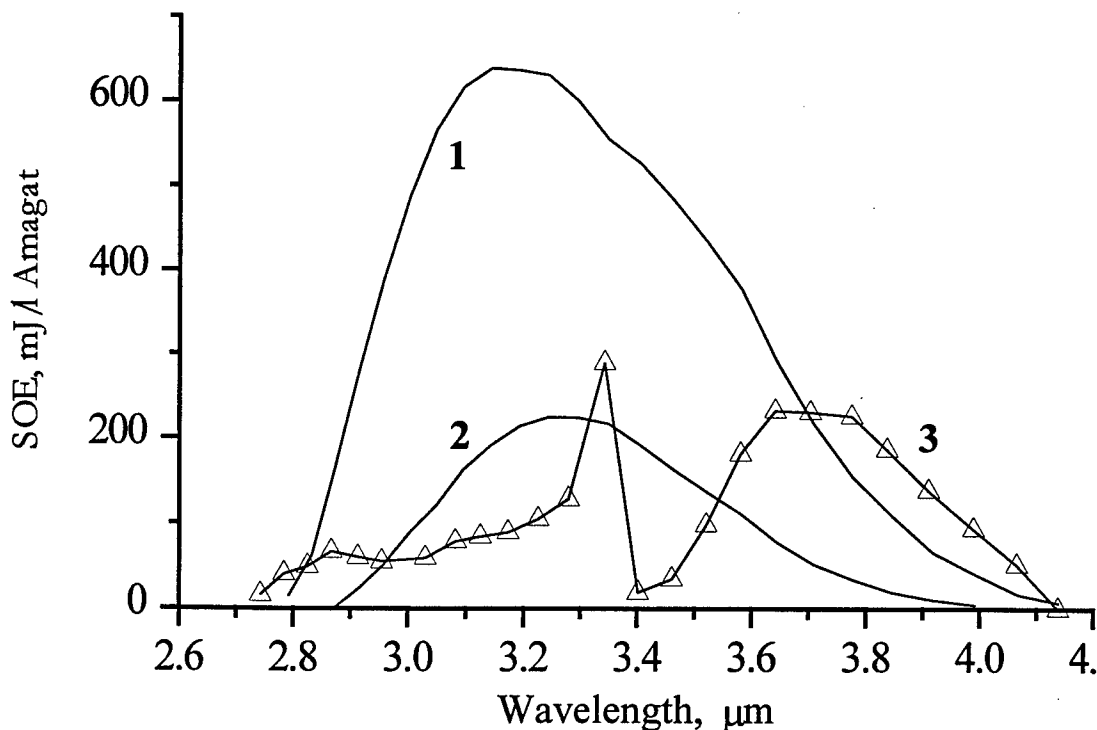
Fig.3.7 Theoretical and experimental (**3**) specific output energy (SOE) vs. wavelength for single line FO CO laser.

Theory data are calculated for different threshold gains 1.75 10^{-3} cm^{-1} (**1**) and 2.00 10^{-3} cm^{-1} (**2**)

3.3.2. Despite the fact that optical characteristics of the laser cavity with diffraction grating are not well known we decided that it is useful to simulate selective lasing in the FO band for conditions close to experimental conditions. Taking as a variable parameter the threshold gain in the selective

cavity calculations were made using our model earlier described. **Fig. 3.9** shows results of calculations of the laser pulse energy in an assumption of selective cavity having the threshold gain independent of wavelength within FO band. Calculated tuning curve is shown for the threshold gain equal to $1.75 \cdot 10^{-3}$ and $2 \cdot 10^{-3}$ cm^{-1}, respectively. Comparison with the experimentally measured tuning curve (**Fig. 3.6**) demonstrates that the position of maximum is different in theory (between 3.0 and 3.6 μm) and in experiment (between 3.7 and 3.9 μm). This discrepancy can be explained in two ways (at present there is not sufficient information to discriminate these two versions). One possible explanation is associated with a probable dependence of the cavity threshold on the wavelength. The second explanation supports the hypothesis already discussed above about the necessity to modify our model by variation of the V-V exchange rate coefficients for the high-lying levels or by introducing multi-quantum exchange processes [12-14].

3.4. Conclusions

The first experiments with pulsed FO CO laser using diffraction grating as a frequency selective element demonstrated a feasibility of a development of frequency tunable single line pulsed FO CO laser. Tunable FO CO lasing on wavelengths from 2.74 up to 4.15 μm corresponding to vibrational transitions from $13 \rightarrow 11$ up to $38 \rightarrow 36$ was obtained. The maximum SOE came up to 0.6 J/l Amagat, single line output efficiency being up to 0.2%. It should be noted that the diffraction gratings used in the experiments were not optimized and further research with other gratings is desirable.

Theoretical prediction for the tuning curve using our model can not be directly compared with experimental data due to the lack of knowledge about cavity losses as a function of the wavelength. However, the comparison of numerical results with available experimental data indicates a necessity of modifying the model to achieve an adequate description of V-V exchange process for high vibrational levels. Theoretical prognosis indicates a feasibility of obtaining high output efficiency for FO CO laser using frequency selective laser resonators and operating on a few (~5) adjacent overtone bands within the spectral range of the FO CO laser. For these conditions, FO CO laser efficiency for the lowest selected transition can reach 3%.

4. References

1. A.A. Ionin, A.A. Kotkov, A.K. Kurnosov, A.P. Napartovich, L.Seleznev et al "Experimental and Theoretical Search of Conditions for Maximum Efficiency and for Frequency Tunability of IR Overtone CO Laser", Scientific Report of Lebedev Institute on Contract SPC-97-4066 with EOARD, pp1-40, Moscow, 1998

2. A.A. Ionin, A.A. Kotkov, A.K. Kurnosov, A.P. Napartovich, L.Seleznev et al, "Pulsed First-Overtone CO Laser: Effective Source of Radiation in Spectral Range of 2.5-4.0 µm", Preprint No.34 of Lebedev Physics Institute, Moscow, 1998 pp. 1-16 (in Russian)

3. A.A. Ionin, A.A. Kotkov, A.K. Kurnosov, A.P. Napartovich, L.Seleznev et al, *Opt. Comm. (1999)* (to be published)

4. N.G. Basov, V.A. Danilychev, A.A. Ionin et al, *Kvantovaya Electronika*, $\underline{5}$, 1833 (1978) (in Russian)

5. N.G. Basov, V.S. Kazakevich, I.B. Kovsh, *Kvantovaya Electronika*, $\underline{7}$, 1966 (1980) (in Russian)

6. N.G. Basov, A.A. Ionin, I.B. Kovsh, *Infrared Physics*, $\underline{25}$, 47 (1985)

7. A. Ionin, A. Kotkov, A. Kurnosov, A. Napartovich, L. Seleznev et al, "Experimental and Theoretical Study on First-Overtone Carbon Monoxide Laser Physics", Scientific Report of Lebedev Institute on Contract SPC-97-4014 with EOARD, pp1-51, Moscow, 1997

8. A.A. Ionin, Yu.M. Klimachev, A.A. Kotkov, A.K. Kurnosov, A.P. Napartovich, L.V. Seleznev et al, "Experimental and Theoretical Study on First-Overtone Carbon Monoxide Laser Physics", Preprint No.11 of Lebedev Physics Institute, Moscow, pp. 1-55 (1998)

9. A.A. Ionin, A.A. Kotkov, A.K. Kurnosov, A.P. Napartovich et al, *Opt. Comm.* $\underline{155}$, (1998), pp. 197-205

10. E. Bachem, A. Dax, T. Fink et al, *Appl. Phys.*, $\underline{B57}$, 185 (1993)

11. M. Murtz et al, *Optics Lett*, $\underline{23}$, 58 (1998)

12. A. Ionin, Yu. Klimachev, Yu. Konev, A. Kurnosov, I. Kochetov, D. Sinitsyn, Proc. Int. Conf. LASERS'97, Dec15-19, 1997, New Orleans, LA, USA; STS.Press, McLEAN, VA, 1998, pp88-91

13. A. Ionin, Yu. Konev, A. Napartovich et al, "Study of vibrational energy exchange and determination of V-V exchange rate constants on high levels of the CO molecule," Interim reports of Lebedev Institute #1 (April-July, 1998) and #2 (August-December, 1998) on Contract SPC-98-4038 with EOARD

14. Yu.M. Klimachev, A.A. Ionin, D.V. Sinitsyn, Yu.B. Konev, A.K. Kurnosov, I.V. Kochetov, Technical Digest of XVI Int. Conf. on Coherent and Nonlinear Optics, June29-July3, 1998, Moscow, Russia, p.112

15. "Diffraction grating handbook (third edition)." Ed. by C. Palmer. Richardson Grating Laboratory, NY, USA, 1996

Appendix I. IR spectrometer for pulsed FO CO laser spectrum measurement

Optical scheme of home-made IR spectrometer is demonstrated in **Fig**. AI.1. Laser radiation I was focused on the slit NS by spherical mirror M1 and directed to the spherical mirror M2 by such a way, that the telescopic mirror system M1+M2 formed a plane parallel wave directed to diffraction grating G. The focal length for mirror M1 and M2 was f_1=0.5 m and f_2=2.5 m, respectively. Therefore, magnification factor was equal 5. As a dispersion element the diffraction grating G (100x100 mm, 150 grooves/mm, λ_{max}=4.0 µm) was used. Spatially separated spectral components of the laser radiation (λ_1 and λ_2 in Fig. A1.1) was focused by spherical mirror M3 onto the screen S situated in the mirror's focal plane. When using the mirror M3 with focal length f_3=5 m, the distance between adjacent vibrational-rotational lines was 5 mm. The spatially and spectrally selected laser radiation focused on the screen was detected by IR video-camera and displayed by TV monitor. The results of vibrational-rotational lines measurement are presented in Chapter 3. When the measurement of vibrational spectrum was only needed (see Chapter 2), spherical mirror M3 with f_3=0.5 m was used. Auxiliary 0.650 µm semiconductor laser radiation was used for calibration of spectral scale on the focal plane of the spectrometer.
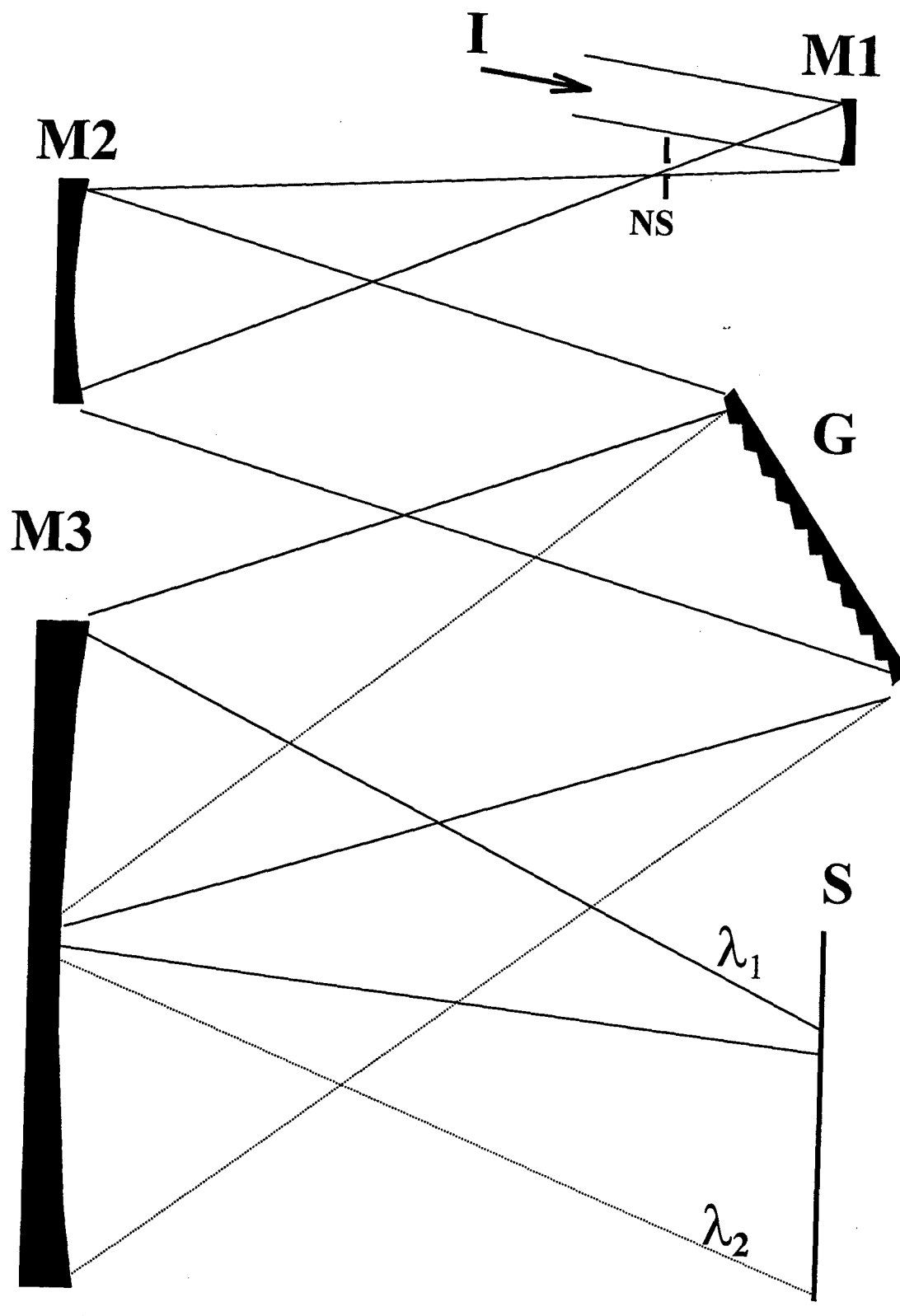
Fig. AI.1 Optical scheme of the home-made spectrometer.

Appendix II. Measurement of transmittance and reflectance of CO laser mirrors

Spectral dependencies for reflection and transmission coefficients of the mirrors manufactured in Rocky Mountain Instrument Co., USA were measured by using Perkin-Elmer 983G IR spectrophotometer. Measurements of the spectral transmission coefficient were performed with the device operating in a standard two-beam mode. When measuring the spectral reflection coefficient, the Perkin-Elmer 3X-Beam Condenser and Specular Reflectance Accessory (3BCSRA) was placed into the channel for a specimen. It allowed us to detect spectra of radiation reflected from a studied object. To work with this accessory it is necessary to calibrate additionally the specimen channel. The specific feature of this procedure is that the calibration factor (so called 100%-Line) varies within the spectral range of interest (1600-4200 cm^{-1}). Its variance is up to $\pm 1.5\%$T (scaled by transparency), and this makes the results of measurements done in a spectrum scanning mode not applicable for calculations of reflection and transmission coefficients with a required accuracy. Obtained in this manner characteristics of the mirrors can be considered only as a qualitative illustration of spectral dependencies of the reflection and transmission coefficients (**Fig. AII.1**).

Therefore, we chose the step by step procedure for spectral measurements with the step equal to 10 or 5 cm^{-1} in dependence on the variation of the measured quantity within the considered spectral interval. The sequence of operations at one step was as follows.

The device was tuned to the given wave number, the zero point was calibrated. Then, using the "Time Drive" mode the following measurements were carried out:

of the level of 100% transmission, $t_0(v)$,

of the transmittance of the mirror under study, $t_{samp}(v)$,

of the signal from the 3BCSRA with the mirror installed, $r_{samp}(v)$,

of the signal when the studied mirror was replaced by the standard one, $r_{st}(v)$.

Then the device was tuned to the next value of the wave number and the cycle of measurements was repeated.

The absolute values of the reflectance $R_{samp}(v)$ and transmittance $T_{samp}(v)$ were found from the relationships:

$$R_{samp}(v) = (r_{samp}(v)/r_{st}(v)) \bullet R_{st}(v),$$

$$T_{samp}(v) = t_{samp}(v)/t_0(v),$$

where $R_{st}(v)$ is the reflectance of the standard mirror measured earlier with a high accuracy [1]. In the proposed methodology the accuracy of measurements is controlled by an absolute error introduced by calibration of zero of the device estimated as 0.05%T. Time interval for each

measurement within the cycle (time of averaging) was taken 20 s. The single-measurement absolute error for these conditions was not higher than 0.005%T, an order of magnitude smaller than the error for calibration of zero of the device.

Taking into account the above described sources of error, the accuracy of measured values for reflectance and transmittance for the studied mirrors is within 0.13%T (for $R_{samp}(v)$) and 0.06%T (for $T_{samp}(v)$). The results of spectral measurements are presented in the **Table AII.1** for lines in the first overtone band and in the **Table AII.2** for spectral lines in the fundamental band.
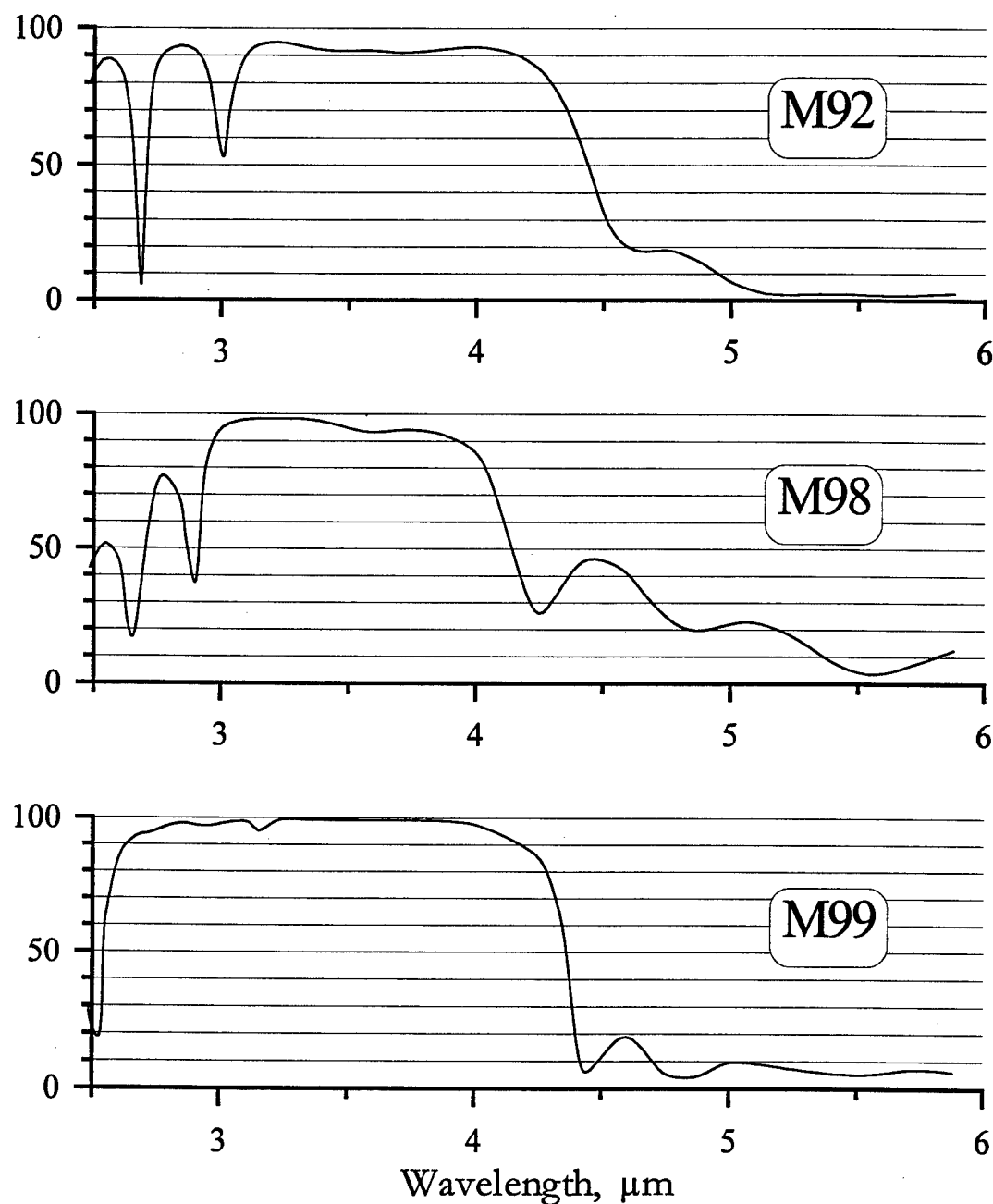
Fig. AII.1. Reflectance of CO laser mirrors used in the experiments

Table AII.1 Measured transmittance and reflectance of dielectric mirrors for calculated wavelength of first overtone CO molecule transitions: V→V-2; J-1→J

V→V-2 V	J-1→J J	Wave-length	M92		M98		M99	
			T%	R%	T%	R%	T%	R%
4	8	2.4252	70.98	28.2	79.85	19.44	65.89	33.67
4	9	2.4277	67.59	31.59	78.72	20.56	63.92	35.65
4	10	2.4303	64.07	35.11	77.52	21.77	62.03	37.56
4	11	2.4329	60.58	38.6	76.31	22.98	60.33	39.29
4	12	2.4356	57.04	42.14	75.07	24.23	58.75	40.88
4	13	2.4384	53.51	45.68	73.8	25.52	57.33	42.32
4	14	2.4411	50.28	48.93	72.61	26.73	56.17	43.5
4	15	2.444	47	52.22	71.35	28.01	55.15	44.53
4	16	2.4468	44	55.23	70.17	29.21	54.38	45.31
4	17	2.4498	40.98	58.25	68.95	30.45	53.8	45.9
4	18	2.4527	38.28	60.95	67.81	31.61	53.48	46.25
5	8	2.4563	35.24	64	66.46	32.97	53.45	46.32
5	9	2.4589	33.25	66	65.52	33.92	53.71	46.08
5	10	2.4616	31.34	67.92	64.59	34.86	54.17	45.62
5	11	2.4643	29.56	69.7	63.69	35.77	54.77	45
5	12	2.467	27.9	71.36	62.82	36.63	55.54	44.22
5	13	2.4698	26.34	72.94	61.97	37.48	56.6	43.17
5	14	2.4726	24.92	74.37	61.16	38.28	57.94	41.86
5	15	2.4755	23.57	75.72	60.35	39.11	59.55	40.26
5	16	2.4784	22.35	76.95	59.54	39.93	61.37	38.41
5	17	2.4814	21.19	78.11	58.74	40.76	63.49	36.26
5	18	2.4844	20.13	79.18	57.97	41.54	65.82	33.9
6	8	2.4883	18.89	80.43	56.99	42.53	69.04	30.69
6	9	2.4909	18.15	81.17	56.35	43.17	71.23	28.5
6	10	2.4936	17.44	81.88	55.73	43.8	73.48	26.14
6	11	2.4963	16.79	82.53	55.15	44.39	75.63	23.74
6	12	2.4991	16.18	83.14	54.58	44.97	77.65	21.49
6	13	2.5019	15.63	83.7	53.99	45.56	79.34	19.74
6	14	2.5048	15.11	84.23	53.38	46.17	80.61	18.55
6	15	2.5078	14.61	84.74	52.78	46.79	81.29	17.98
6	16	2.5107	14.16	85.2	52.23	47.37	81.26	18.13
6	17	2.5138	13.74	85.65	51.7	47.94	80.38	19.1
6	18	2.5169	13.35	86.05	51.21	48.46	78.65	20.91
7	8	2.5209	12.92	86.5	50.58	49.11	75.25	24.37
7	9	2.5236	12.65	86.77	50.19	49.52	72.36	27.29
7	10	2.5263	12.42	87.02	49.83	49.88	69.16	30.58
7	11	2.5291	12.21	87.24	49.51	50.22	65.59	34.22
7	12	2.532	12	87.46	49.19	50.54	61.66	38.07
7	13	2.5349	11.82	87.66	48.89	50.85	57.61	41.9
7	14	2.5378	11.66	87.84	48.64	51.12	53.65	45.71
7	15	2.5408	11.53	87.98	48.46	51.33	49.83	49.59
7	16	2.5438	11.43	88.09	48.31	51.5	46.24	53.23

V→V-2 V	J-1→J J	Wave-length	M92		M98		M99	
			T%	R%	T%	R%	T%	R%
7	17	2.5469	11.34	88.19	48.18	51.64	42.71	56.61
7	18	2.5501	11.26	88.28	48.11	51.73	39.33	59.78
8	8	2.5544	11.19	88.38	48.17	51.69	35.34	63.73
8	9	2.5571	11.18	88.4	48.26	51.61	33.16	66.04
8	10	2.5599	11.22	88.38	48.38	51.49	31.14	68.25
8	11	2.5627	11.28	88.33	48.55	51.31	29.25	70.19
8	12	2.5656	11.34	88.28	48.8	51.06	27.33	71.82
8	13	2.5686	11.41	88.21	49.13	50.71	25.45	73.28
8	14	2.5716	11.52	88.1	49.55	50.27	23.85	74.79
8	15	2.5746	11.67	87.95	50.05	49.75	22.53	76.37
8	16	2.5777	11.86	87.76	50.64	49.15	21.3	77.79
8	17	2.5808	12.07	87.55	51.32	48.48	20.12	78.9
8	18	2.584	12.33	87.29	52.11	47.67	18.99	79.89
9	8	2.5886	12.77	86.82	53.48	46.28	17.57	81.23
9	9	2.5914	13.09	86.49	54.44	45.29	16.77	82
9	10	2.5942	13.44	86.12	55.49	44.23	16.02	82.72
9	11	2.5971	13.83	85.7	56.58	43.12	15.32	83.41
9	12	2.6001	14.29	85.21	57.7	41.97	14.68	84.06
9	13	2.6031	14.82	84.65	59	40.65	14.08	84.64
9	14	2.6061	15.43	84.01	60.6	39.03	13.48	85.17
9	15	2.6092	16.14	83.29	62.37	37.24	12.89	85.69
9	16	2.6124	16.92	82.49	64.02	35.58	12.38	86.27
9	17	2.6156	17.81	81.61	65.61	33.97	11.93	86.85
9	18	2.6189	18.92	80.51	67.58	31.98	11.46	87.34
10	8	2.6237	20.82	78.61	70.78	28.74	10.78	87.92
10	9	2.6265	22	77.41	72.37	27.13	10.46	88.31
10	10	2.6294	23.38	76.02	73.9	25.58	10.17	88.71
10	11	2.6323	25.05	74.33	75.56	23.88	9.844	89.01
10	12	2.6353	27.1	72.25	77.4	22	9.469	89.23
10	13	2.6384	29.42	69.9	79.1	20.28	9.127	89.49
10	14	2.6415	31.87	67.42	80.36	18.99	8.878	89.84
10	15	2.6447	34.69	64.55	81.39	17.96	8.662	90.19
10	16	2.6479	37.98	61.21	82.28	17.08	8.432	90.44
10	17	2.6512	42.05	57.11	82.89	16.48	8.182	90.64
10	18	2.6545	46.9	52.25	83.01	16.39	7.938	90.86
11	8	2.6596	55.03	44.1	82.38	17.03	7.645	91.24
11	9	2.6625	59.71	39.42	81.68	17.7	7.54	91.44
11	10	2.6654	65.06	34.09	80.57	18.76	7.432	91.58
11	11	2.6684	71.8	27.39	78.85	20.43	7.274	91.64
11	12	2.6715	79.19	20.06	76.64	22.61	7.08	91.67
11	13	2.6746	85.52	13.77	74.29	24.94	6.906	91.76
11	14	2.6778	90.15	9.174	71.84	27.41	6.757	91.93
11	15→J	2.681	92.76	6.602	69.24	30.04	6.612	92.07
11	16	2.6843	93.3	6.1	66.4	32.94	6.457	92.13

V→V-2 V	J-1→J J	Wave-length	M92		M98		M99	
			T%	R%	T%	R%	T%	R%
11	17	2.6876	91.7	7.746	63.58	35.83	6.334	92.22
11	18	2.691	87.83	11.63	60.81	38.64	6.264	92.4
12	8	2.6964	77.43	22.05	56.16	43.37	6.134	92.6
12	9	2.6993	70.44	29.05	53.46	46.1	6.025	92.61
12	10	2.7023	63.51	35.98	50.84	48.68	5.931	92.63
12	11	2.7054	57.42	42.06	48.52	50.89	5.882	92.71
12	12	2.7085	51.92	47.54	46.54	52.91	5.85	92.76
12	13	2.7117	46.19	53.22	44.75	55.14	5.796	92.65
12	14	2.7149	40.67	58.68	42.98	57.4	5.725	92.45
12	15	2.7182	35.91	63.38	40.87	59.49	5.661	92.31
12	16	2.7215	32.2	67.04	38.54	61.26	5.597	92.27
12	17	2.725	28.79	70.41	36.28	63.02	5.478	92.26
12	18	2.7284	25.69	73.46	34.55	64.7	5.315	92.24
13	8	2.7341	21.86	77.27	32.44	66.94	5.193	92.26
13	9	2.7371	20.44	78.7	31.47	67.87	5.193	92.29
13	10	2.7401	18.92	80.23	30.38	68.91	5.114	92.27
13	11	2.7433	17.1	82.03	29.1	70.17	4.925	92.19
13	12	2.7464	15.58	83.53	28.03	71.22	4.743	92.14
13	13	2.7497	14.59	84.52	27.3	71.92	4.64	92.17
13	14	2.753	13.91	85.18	26.78	72.42	4.576	92.21
13	15	2.7563	13.1	85.97	26.16	73.02	4.467	92.15
13	16	2.7598	12.1	86.94	25.38	73.77	4.301	91.98
13	17	2.7632	11.27	87.75	24.74	74.41	4.137	91.79
13	18	2.7668	10.63	88.38	24.26	74.89	3.981	91.61
14	8	2.7727	9.768	89.19	23.66	75.48	3.703	91.38
14	9	2.7758	9.353	89.58	23.41	75.72	3.558	91.29
14	10	2.7789	8.996	89.91	23.22	75.9	3.442	91.21
14	11	2.7821	8.676	90.23	23.09	76.03	3.345	91.13
14	12	2.7853	8.36	90.54	23	76.12	3.238	91.03
14	13	2.7886	8.022	90.87	22.94	76.18	3.103	90.92
14	14	2.792	7.732	91.16	22.96	76.17	2.975	90.86
14	15	2.7954	7.561	91.33	23.09	76.04	2.891	90.9
14	16	2.7989	7.436	91.45	23.3	75.83	2.824	90.99
14	17	2.8025	7.232	91.66	23.53	75.6	2.722	91.08
14	18	2.8061	6.973	91.92	23.79	75.35	2.595	91.15
15	8	2.8123	6.726	92.17	24.52	74.63	2.445	91.35
15	9	2.8155	6.672	92.23	25.04	74.11	2.399	91.49
15	10	2.8187	6.587	92.32	25.65	73.52	2.347	91.61
15	11	2.8219	6.485	92.43	26.32	72.87	2.292	91.73
15	12	2.8252	6.41	92.53	27.09	72.13	2.245	91.89
15	13	2.8286	6.38	92.58	27.98	71.27	2.209	92.11
15	14	2.832	6.36	92.63	29	70.28	2.171	92.33
15	15	2.8355	6.319	92.7	30.22	69.09	2.118	92.51
15	16	2.8391	6.276	92.76	31.64	67.68	2.063	92.69

| V→V-2 | J-1→J | Wave- | M92 | | M98 | | M99 | |
V	J	length	T%	R%	T%	R%	T%	R%
15	17	2.8427	6.269	92.78	33.23	66.09	2.023	92.9
15	18	2.8464	6.295	92.76	35.05	64.25	1.999	93.14
16	8	2.853	6.35	92.67	38.9	60.29	1.969	93.52
16	9	2.8562	6.388	92.59	41.06	58.05	1.96	93.69
16	10	2.8594	6.446	92.5	43.39	55.63	1.958	93.87
16	11	2.8627	6.519	92.38	45.96	52.96	1.964	94.05
16	12	2.8661	6.595	92.25	48.73	50.1	1.977	94.23
16	13	2.8696	6.679	92.11	51.64	47.09	1.995	94.41
16	14	2.8731	6.794	91.95	54.53	44.14	2.012	94.58
16	15	2.8766	6.954	91.77	57.26	41.37	2.023	94.73
16	16	2.8803	7.144	91.57	59.75	38.86	2.029	94.88
16	17	2.884	7.327	91.38	61.6	37.01	2.033	94.99
16	18	2.8877	7.516	91.2	62.62	36	2.047	95.08
17	8	2.8947	7.98	90.77	61.79	36.87	2.138	95.19
17	9	2.8979	8.225	90.55	60.12	38.58	2.193	95.19
17	10	2.9012	8.483	90.32	57.57	41.18	2.243	95.15
17	11	2.9046	8.774	90.06	54.29	44.51	2.29	95.07
17	12	2.9081	9.124	89.75	50.54	48.32	2.336	94.95
17	13	2.9116	9.527	89.38	46.59	52.32	2.385	94.81
17	14	2.9152	9.975	88.97	42.46	56.48	2.439	94.62
17	15	2.9188	10.45	88.52	38.41	60.57	2.498	94.38
17	16	2.9225	11	88	34.45	64.55	2.56	94.12
17	17	2.9263	11.65	87.36	30.73	68.29	2.62	93.86
17	18	2.9301	12.4	86.63	27.38	71.63	2.676	93.58
18	8	2.9375	14.05	85	21.96	77.04	2.783	92.85
18	9	2.9408	14.9	84.15	19.93	79.06	2.826	92.5
18	10	2.9442	15.88	83.16	18.05	80.93	2.862	92.16
18	11	2.9476	16.98	82.05	16.37	82.59	2.885	91.85
18	12	2.9511	18.25	80.78	14.86	84.08	2.891	91.56
18	13	2.9547	19.7	79.31	13.51	85.42	2.88	91.29
18	14	2.9584	21.35	77.65	12.3	86.62	2.855	91.05
18	15	2.9621	23.17	75.83	11.22	87.68	2.822	90.84
18	16	2.9659	25.24	73.76	10.24	88.66	2.778	90.66
18	17	2.9697	27.52	71.49	9.384	89.52	2.722	90.54
18	18	2.9737	30.15	68.87	8.593	90.33	2.647	90.48
19	8	2.9814	35.77	63.32	7.332	91.68	2.45	90.66
19	9	2.9848	38.29	60.83	6.861	92.2	2.367	90.86
19	10	2.9882	40.71	58.46	6.432	92.68	2.299	91.12
19	11	2.9917	42.95	56.25	6.033	93.13	2.236	91.42
19	12	2.9953	44.88	54.36	5.665	93.54	2.168	91.71
19	13	2.999	46.32	52.95	5.328	93.91	2.093	91.99
19	14	3.0027	47.05	52.24	5.025	94.24	2.019	92.26
19	15	3.0065	46.96	52.35	4.742	94.54	1.949	92.53
19	16	3.0104	46.04	53.27	4.479	94.82	1.875	92.81

V→V-2 V	J-1→J J	Wave-length	M92		M98		M99	
			T%	R%	T%	R%	T%	R%
19	17	3.0143	44.4	54.91	4.242	95.07	1.795	93.11
19	18	3.0184	42.07	57.26	4.016	95.32	1.712	93.43
20	8	3.0265	36.4	62.95	3.63	95.76	1.611	94.01
20	9	3.0299	33.9	65.46	3.492	95.92	1.587	94.24
20	10	3.0334	31.42	67.96	3.365	96.07	1.564	94.46
20	11	3.037	29.01	70.4	3.249	96.2	1.541	94.67
20	12	3.0407	26.71	72.73	3.14	96.33	1.516	94.86
20	13	3.0445	24.54	74.91	3.035	96.46	1.49	95.04
20	14	3.0483	22.58	76.9	2.928	96.58	1.468	95.22
20	15	3.0522	20.76	78.74	2.815	96.71	1.453	95.43
20	16	3.0561	19.14	80.38	2.708	96.83	1.449	95.63
20	17	3.0602	17.63	81.91	2.615	96.94	1.458	95.79
20	18	3.0643	16.3	83.25	2.539	97.03	1.473	95.91
21	8	3.0728	13.96	85.61	2.398	97.21	1.487	96.16
21	9	3.0763	13.15	86.43	2.346	97.27	1.49	96.25
21	10	3.0799	12.4	87.19	2.298	97.34	1.499	96.3
21	11	3.0836	11.72	87.88	2.253	97.39	1.517	96.33
21	12	3.0873	11.11	88.5	2.209	97.44	1.545	96.35
21	13	3.0912	10.53	89.09	2.163	97.49	1.587	96.38
21	14	3.0951	10.01	89.61	2.12	97.54	1.64	96.4
21	15	3.099	9.525	90.09	2.08	97.58	1.705	96.4
21	16	3.1031	9.059	90.55	2.043	97.62	1.785	96.38
21	17	3.1072	8.636	90.96	2.011	97.64	1.88	96.33
21	18	3.1114	8.247	91.34	1.979	97.66	1.993	96.25
22	8	3.1204	7.554	92.01	1.87	97.76	2.282	95.97
22	9	3.124	7.306	92.25	1.821	97.81	2.426	95.78
22	10	3.1277	7.055	92.5	1.779	97.85	2.602	95.51
22	11	3.1314	6.82	92.75	1.747	97.89	2.817	95.18
22	12	3.1352	6.614	92.96	1.722	97.92	3.092	94.77
22	13	3.1392	6.441	93.14	1.702	97.95	3.44	94.27
22	14	3.1431	6.294	93.3	1.683	97.97	3.816	93.69
22	15	3.1472	6.142	93.45	1.66	97.98	4.22	92.95
22	16	3.1513	6	93.59	1.638	97.98	4.575	92.17
22	17	3.1556	5.881	93.71	1.626	97.97	4.821	91.44
22	18	3.1599	5.793	93.8	1.624	97.95	4.889	90.91
23	8	3.1693	5.595	93.96	1.598	97.92	4.371	90.95
23	9	3.173	5.514	94.02	1.582	97.93	3.986	91.37
23	10	3.1767	5.445	94.08	1.573	97.94	3.568	91.9
23	11	3.1806	5.388	94.13	1.57	97.95	3.129	92.53
23	12	3.1845	5.343	94.18	1.57	97.96	2.719	93.18
23	13	3.1885	5.307	94.22	1.572	97.98	2.352	93.81
23	14	3.1926	5.278	94.26	1.571	98	2.033	94.41
23	15	3.1967	5.254	94.3	1.566	98.03	1.771	94.95
23	16	3.201	5.233	94.34	1.556	98.05	1.548	95.45

V→V-2 V	J-1→J J	Wave-length	M92 T%	M92 R%	M98 T%	M98 R%	M99 T%	M99 R%
23	17	3.2053	5.216	94.37	1.549	98.06	1.367	95.86
23	18	3.2097	5.205	94.39	1.546	98.07	1.215	96.2
24	8	3.2196	5.203	94.41	1.558	98.09	0.966	96.85
24	9	3.2234	5.208	94.42	1.561	98.1	0.8951	97.07
24	10	3.2272	5.213	94.43	1.557	98.13	0.8323	97.26
24	11	3.2311	5.22	94.44	1.55	98.16	0.7764	97.42
24	12	3.2352	5.239	94.44	1.55	98.19	0.731	97.57
24	13	3.2392	5.275	94.42	1.564	98.2	0.7013	97.7
24	14	3.2434	5.323	94.4	1.587	98.2	0.6763	97.83
24	15	3.2477	5.369	94.37	1.608	98.2	0.6445	97.97
24	16	3.252	5.408	94.35	1.619	98.21	0.605	98.1
24	17	3.2564	5.45	94.33	1.62	98.22	0.5699	98.2
24	18	3.2609	5.501	94.29	1.612	98.23	0.5503	98.27
25	8	3.2714	5.639	94.18	1.658	98.2	0.5337	98.41
25	9	3.2752	5.696	94.12	1.698	98.17	0.5263	98.49
25	10	3.2792	5.768	94.05	1.728	98.14	0.5158	98.55
25	11	3.2832	5.85	93.97	1.737	98.14	0.5021	98.6
25	12	3.2873	5.929	93.88	1.733	98.14	0.4854	98.65
25	13	3.2915	5.993	93.82	1.724	98.14	0.4664	98.7
25	14	3.2957	6.049	93.76	1.723	98.14	0.4493	98.75
25	15	3.3001	6.125	93.68	1.746	98.11	0.4391	98.79
25	16	3.3045	6.234	93.57	1.796	98.05	0.4388	98.81
25	17	3.3091	6.359	93.44	1.85	97.99	0.4405	98.82
25	18	3.3137	6.47	93.32	1.875	97.96	0.4352	98.84
26	8	3.3247	6.704	93.09	1.913	97.92	0.4181	98.94
26	9	3.3286	6.793	93	1.951	97.88	0.4191	98.97
26	10	3.3326	6.885	92.91	1.992	97.85	0.42	98.98
26	11	3.3367	6.98	92.82	2.029	97.82	0.4179	99
26	12	3.3409	7.074	92.73	2.065	97.79	0.4134	99.02
26	13	3.3452	7.165	92.64	2.108	97.75	0.4078	99.04
26	14	3.3496	7.255	92.55	2.161	97.7	0.4027	99.07
26	15	3.3541	7.355	92.45	2.213	97.65	0.4	99.09
26	16	3.3586	7.469	92.34	2.257	97.6	0.4016	99.09
26	17	3.3632	7.587	92.22	2.296	97.55	0.4064	99.08
26	18	3.368	7.687	92.11	2.338	97.5	0.4125	99.08
27	8	3.3796	7.869	91.92	2.484	97.34	0.4199	99.1
27	9	3.3836	7.945	91.84	2.549	97.27	0.4188	99.11
27	10	3.3877	8.021	91.77	2.614	97.22	0.4192	99.12
27	11	3.3919	8.084	91.71	2.669	97.16	0.4239	99.13
27	12	3.3962	8.134	91.66	2.721	97.12	0.4298	99.14
27	13	3.4006	8.183	91.62	2.784	97.07	0.4297	99.15
27	14	3.4051	8.235	91.57	2.87	97	0.4198	99.17
27	15	3.4096	8.282	91.53	2.968	96.93	0.4103	99.19
27	16	3.4143	8.312	91.51	3.069	96.83	0.4148	99.23

V→V-2 V	J-1→J J	Wave-length	M92		M98		M99	
			T%	R%	T%	R%	T%	R%
27	17	3.419	8.326	91.5	3.165	96.72	0.4334	99.27
27	18	3.4239	8.341	91.49	3.265	96.6	0.4505	99.3
28	8	3.4361	8.401	91.41	3.512	96.3	0.4387	99.33
28	9	3.4403	8.398	91.4	3.583	96.21	0.432	99.34
28	10	3.4445	8.39	91.4	3.66	96.11	0.4292	99.35
28	11	3.4488	8.393	91.38	3.758	96	0.4315	99.35
28	12	3.4532	8.412	91.36	3.884	95.87	0.4389	99.33
28	13	3.4577	8.428	91.33	4.024	95.73	0.4476	99.31
28	14	3.4623	8.424	91.33	4.161	95.6	0.4536	99.31
28	15	3.4669	8.402	91.34	4.288	95.48	0.4569	99.31
28	16	3.4717	8.378	91.36	4.412	95.36	0.4605	99.31
28	17	3.4766	8.366	91.37	4.534	95.24	0.4669	99.31
28	18	3.4815	8.361	91.38	4.655	95.12	0.476	99.3
29	8	3.4945	8.342	91.4	4.993	94.77	0.4999	99.27
29	9	3.4987	8.333	91.41	5.109	94.66	0.4975	99.27
29	10	3.503	8.322	91.43	5.23	94.55	0.4917	99.27
29	11	3.5074	8.311	91.45	5.35	94.45	0.4897	99.28
29	12	3.5119	8.299	91.47	5.469	94.35	0.4982	99.3
29	13	3.5165	8.287	91.5	5.583	94.26	0.515	99.33
29	14	3.5212	8.278	91.53	5.696	94.17	0.5344	99.34
29	15	3.526	8.273	91.54	5.805	94.08	0.5529	99.34
29	16	3.5309	8.265	91.56	5.908	93.99	0.5727	99.33
29	17	3.5359	8.247	91.59	6.001	93.91	0.5964	99.32
29	18	3.541	8.227	91.61	6.087	93.83	0.6221	99.29
30	8	3.5547	8.248	91.56	6.295	93.55	0.6697	99.12
30	9	3.559	8.264	91.53	6.36	93.45	0.6853	99.09
30	10	3.5634	8.275	91.52	6.424	93.37	0.7059	99.1
30	11	3.5679	8.284	91.51	6.478	93.32	0.7284	99.1
30	12	3.5726	8.296	91.49	6.513	93.29	0.7492	99.09
30	13	3.5773	8.314	91.48	6.525	93.29	0.7668	99.05
30	14	3.5821	8.335	91.45	6.529	93.3	0.7853	99.01
30	15	3.587	8.359	91.43	6.538	93.3	0.8084	98.99
30	16	3.592	8.386	91.41	6.548	93.28	0.836	99
30	17	3.5971	8.416	91.38	6.549	93.28	0.866	99
30	18	3.6024	8.45	91.35	6.531	93.29	0.8943	98.97
31	8	3.6168	8.53	91.25	6.472	93.34	0.8887	98.91
31	9	3.6212	8.554	91.23	6.462	93.34	0.8725	98.91
31	10	3.6258	8.585	91.19	6.453	93.34	0.8648	98.92
31	11	3.6304	8.62	91.15	6.442	93.35	0.8636	98.94
31	12	3.6351	8.658	91.11	6.421	93.37	0.8603	98.96
31	13	3.64	8.699	91.07	6.384	93.41	0.8473	98.96
31	14	3.6449	8.74	91.03	6.34	93.47	0.8269	98.96
31	15	3.65	8.782	90.99	6.3	93.51	0.8036	98.98
31	16	3.6551	8.822	90.95	6.27	93.53	0.7815	99.02

V→V-2	J-1→J	Wave-	M92		M98		M99	
V	J	length	T%	R%	T%	R%	T%	R%
31	17	3.6604	8.86	90.92	6.234	93.56	0.7576	99.06
31	18	3.6657	8.892	90.89	6.178	93.61	0.7304	99.08
32	8	3.681	8.968	90.8	6.048	93.74	0.6844	99.09
32	9	3.6856	8.993	90.77	6.044	93.75	0.6834	99.11
32	10	3.6902	9.016	90.74	6.037	93.75	0.6775	99.13
32	11	3.695	9.041	90.72	6.016	93.77	0.6638	99.15
32	12	3.6998	9.065	90.69	5.987	93.8	0.6519	99.16
32	13	3.7048	9.092	90.67	5.957	93.83	0.6525	99.14
32	14	3.7099	9.117	90.65	5.933	93.86	0.6665	99.11
32	15	3.7151	9.13	90.64	5.921	93.88	0.6791	99.09
32	16	3.7203	9.123	90.66	5.924	93.88	0.6754	99.12
32	17	3.7257	9.103	90.69	5.936	93.89	0.6599	99.18
32	18	3.7312	9.089	90.72	5.939	93.9	0.6493	99.24
33	8	3.7474	9.08	90.77	5.898	93.98	0.6562	99.24
33	9	3.7521	9.053	90.8	5.904	93.98	0.6448	99.25
33	10	3.7569	9.02	90.84	5.916	93.96	0.6326	99.26
33	11	3.7618	8.986	90.88	5.93	93.93	0.6268	99.25
33	12	3.7667	8.953	90.92	5.948	93.91	0.6274	99.21
33	13	3.7718	8.916	90.95	5.975	93.88	0.6298	99.18
33	14	3.777	8.87	90.99	6.016	93.83	0.6298	99.18
33	15	3.7824	8.814	91.04	6.064	93.79	0.6287	99.19
33	16	3.7878	8.746	91.1	6.107	93.74	0.6308	99.2
33	17	3.7933	8.668	91.18	6.142	93.71	0.6382	99.2
33	18	3.799	8.588	91.27	6.181	93.67	0.6472	99.19
34	8	3.8162	8.416	91.44	6.397	93.45	0.6717	99.19
34	9	3.821	8.373	91.49	6.464	93.38	0.6919	99.18
34	10	3.8259	8.324	91.54	6.533	93.31	0.7146	99.15
34	11	3.8309	8.262	91.6	6.61	93.23	0.7314	99.13
34	12	3.836	8.186	91.68	6.697	93.15	0.7368	99.1
34	13	3.8412	8.105	91.76	6.791	93.07	0.7374	99.08
34	14	3.8466	8.03	91.84	6.887	92.99	0.7425	99.08
34	15	3.852	7.969	91.91	6.981	92.9	0.7577	99.11
34	16	3.8576	7.913	91.97	7.084	92.8	0.78	99.13
34	17	3.8633	7.854	92.03	7.206	92.67	0.8048	99.12
34	18	3.8691	7.787	92.09	7.35	92.52	0.8267	99.08
35	8	3.8874	7.527	92.33	7.899	91.95	0.851	98.95
35	9	3.8923	7.481	92.37	8.057	91.78	0.873	98.93
35	10	3.8973	7.453	92.39	8.219	91.6	0.9113	98.91
35	11	3.9025	7.428	92.41	8.391	91.42	0.9577	98.89
35	12	3.9077	7.387	92.45	8.569	91.24	0.9999	98.85
35	13	3.9131	7.328	92.51	8.767	91.04	1.037	98.8
35	14	3.9186	7.267	92.57	8.989	90.83	1.076	98.74
35	15	3.9242	7.223	92.62	9.248	90.58	1.124	98.68
35	16	3.93	7.197	92.65	9.544	90.29	1.186	98.62

V→V-2 V	J-1→J J	Wave-length	M92		M98		M99	
			T%	R%	T%	R%	T%	R%
35	17	3.9358	7.18	92.68	9.856	89.98	1.259	98.57
35	18	3.9418	7.161	92.71	10.19	89.67	1.347	98.52
36	8	3.9612	7.074	92.82	11.37	88.54	1.698	98.23
36	9	3.9663	7.061	92.84	11.72	88.2	1.795	98.13
36	10	3.9715	7.063	92.84	12.11	87.82	1.888	98.03
36	11	3.9767	7.075	92.83	12.51	87.42	1.98	97.94
36	12	3.9821	7.089	92.82	12.94	86.99	2.083	97.85
36	13	3.9877	7.094	92.82	13.41	86.52	2.208	97.73
36	14	3.9933	7.097	92.81	13.91	86.02	2.351	97.59
36	15	3.9991	7.111	92.8	14.48	85.45	2.518	97.42
36	16	4.005	7.145	92.77	15.11	84.82	2.703	97.23
36	17	4.011	7.187	92.74	15.8	84.13	2.904	97.01
36	18	4.0172	7.22	92.71	16.57	83.36	3.122	96.79
37	8	4.0379	7.353	92.58	19.48	80.45	3.938	96.01
37	9	4.0431	7.42	92.51	20.3	79.62	4.165	95.79
37	10	4.0484	7.48	92.44	21.19	78.72	4.392	95.55
37	11	4.0538	7.526	92.39	22.16	77.74	4.618	95.3
37	12	4.0594	7.569	92.34	23.23	76.66	4.857	95.02
37	13	4.0651	7.623	92.28	24.4	75.49	5.119	94.74
37	14	4.0709	7.699	92.19	25.68	74.21	5.409	94.45
37	15	4.0768	7.794	92.09	27.06	72.83	5.71	94.18
37	16	4.0829	7.907	91.97	28.54	71.34	6.005	93.9
37	17	4.0891	8.03	91.84	30.12	69.76	6.277	93.64
37	18	4.0954	8.156	91.71	31.8	68.07	6.531	93.38
38	8	4.1175	8.603	91.23	38.46	61.36	7.363	92.44
38	9	4.1229	8.746	91.08	40.27	59.54	7.57	92.24
38	10	4.1283	8.9	90.92	42.13	57.66	7.772	92.04
38	11	4.1339	9.064	90.75	44.11	55.66	7.968	91.83
38	12	4.1396	9.235	90.57	46.18	53.58	8.155	91.61
38	13	4.1455	9.421	90.38	48.38	51.38	8.349	91.38
38	14	4.1515	9.625	90.17	50.66	49.09	8.558	91.18
38	15	4.1576	9.849	89.94	53.01	46.72	8.79	90.99
38	16	4.1639	10.1	89.69	55.43	44.28	9.045	90.79
38	17	4.1703	10.36	89.41	57.87	41.83	9.317	90.53
38	18	4.1768	10.65	89.11	60.27	39.4	9.606	90.24
39	8	4.2004	11.79	87.89	67.83	31.69	10.83	89.04
39	9	4.2059	12.1	87.55	69.19	30.3	11.18	88.68
39	10	4.2115	12.43	87.18	70.38	29.08	11.58	88.27
39	11	4.2173	12.79	86.79	71.42	28.02	12.01	87.82
39	12	4.2232	13.14	86.4	72.29	27.15	12.47	87.35
39	13	4.2292	13.51	86.01	73.01	26.43	12.95	86.85
39	14	4.2354	13.9	85.6	73.64	25.82	13.47	86.29
39	15	4.2417	14.32	85.17	74.17	25.31	14.03	85.67
39	16	4.2481	14.8	84.69	74.54	24.96	14.64	84.99

V→V-2 V	J-1→J J	Wave-length	M92		M98		M99	
			T%	R%	T%	R%	T%	R%
39	17	4.2547	15.34	84.16	74.62	24.91	15.35	84.22
39	18	4.2614	15.96	83.56	74.33	25.23	16.19	83.37
40	8	4.2867	18.46	81.15	71.87	27.75	20.31	79.27
40	9	4.2924	19.09	80.53	71.19	28.43	21.48	78.1
40	10	4.2982	19.79	79.84	70.43	29.19	22.78	76.82
40	11	4.3041	20.55	79.09	69.61	30.02	24.23	75.38
40	12	4.3102	21.37	78.27	68.7	30.93	25.88	73.74
40	13	4.3164	22.24	77.4	67.75	31.89	27.71	71.89
40	14	4.3228	23.18	76.47	66.76	32.9	29.78	69.79
40	15	4.3293	24.18	75.48	65.75	33.92	32.09	67.44
40	16	4.3359	25.25	74.42	64.76	34.94	34.66	64.84
40	17	4.3427	26.41	73.28	63.77	35.96	37.54	61.94
40	18	4.3497	27.67	72.05	62.79	36.97	40.75	58.7

Table AII.2 Measured transmittance and reflectance of dielectric mirrors for calculated wavelength of fundamental band CO molecule transitions: V→V-1; J-1→J

| V→V-1 | J-1→J | Wave- | M92 | | M98 | | M99 | |
V	J	length	T%	R%	T%	R%	T%	R%
3	7	4.8454	84.13	15.21	80.19	19.25	95.65	3.059
3	8	4.8548	84.58	14.77	80.35	19.08	95.37	3.354
3	9	4.8644	85.01	14.35	80.45	18.97	95.08	3.658
3	10	4.8741	85.51	13.85	80.51	18.91	94.71	4.034
3	11	4.8839	86.05	13.32	80.5	18.91	94.29	4.449
3	12	4.8938	86.59	12.77	80.43	18.97	93.84	4.885
3	13	4.9038	87.13	12.22	80.3	19.09	93.39	5.319
3	14	4.914	87.66	11.69	80.14	19.25	92.96	5.737
4	7	4.9075	87.29	12.06	80.26	19.13	93.26	5.446
4	8	4.9171	87.83	11.52	80.08	19.3	92.84	5.86
4	9	4.9268	88.4	10.94	79.9	19.5	92.47	6.262
4	10	4.9366	89.02	10.32	79.7	19.69	92.13	6.651
4	11	4.9466	89.63	9.716	79.51	19.89	91.83	7.011
4	12	4.9567	90.18	9.18	79.31	20.09	91.55	7.328
4	13	4.9669	90.71	8.666	79.11	20.3	91.29	7.601
4	14	4.9773	91.31	8.085	78.87	20.55	91.07	7.833
5	7	4.971	90.94	8.446	79.01	20.39	91.2	7.698
5	8	4.9808	91.58	7.822	78.76	20.65	90.99	7.915
5	9	4.9907	92.29	7.123	78.48	20.94	90.81	8.096
5	10	5.0007	93	6.422	78.22	21.22	90.67	8.243
5	11	5.0108	93.65	5.779	77.98	21.47	90.57	8.353
5	12	5.0211	94.2	5.221	77.78	21.69	90.52	8.42
5	13	5.0315	94.64	4.769	77.64	21.87	90.51	8.439
5	14	5.042	95.04	4.362	77.53	22.01	90.54	8.416
6	7	5.036	94.83	4.576	77.58	21.94	90.52	8.432
6	8	5.0459	95.17	4.224	77.5	22.05	90.55	8.402
6	9	5.056	95.51	3.878	77.44	22.13	90.61	8.362
6	10	5.0662	95.85	3.533	77.42	22.17	90.68	8.312
6	11	5.0765	96.2	3.178	77.41	22.17	90.77	8.229
6	12	5.087	96.49	2.894	77.44	22.13	90.87	8.127
6	13	5.0975	96.76	2.619	77.51	22.05	90.97	8.013
6	14	5.1083	96.98	2.398	77.61	21.93	91.07	7.931
7	7	5.1025	96.87	2.505	77.55	21.99	91.02	7.97
7	8	5.1127	97.08	2.297	77.68	21.87	91.13	7.89
7	9	5.1229	97.27	2.113	77.84	21.71	91.27	7.768
7	10	5.1333	97.43	1.95	78.04	21.52	91.48	7.555
7	11	5.1438	97.58	1.797	78.29	21.27	91.67	7.333
7	12	5.1544	97.69	1.681	78.56	21.01	91.63	7.355
7	13	5.1652	97.79	1.58	78.91	20.67	91.3	7.714
7	14	5.1761	97.88	1.503	79.28	20.29	91.04	8.019
8	7	5.1707	97.84	1.535	79.11	20.47	91.12	7.919

V→V-1 V	J-1→J J	Wave-length	M92 T%	M92 R%	M98 T%	M98 R%	M99 T%	M99 R%
8	8	5.181	97.91	1.474	79.46	20.12	91.07	8.004
8	9	5.1914	97.96	1.425	79.83	19.76	91.49	7.612
8	10	5.2019	98	1.384	80.27	19.31	92.16	6.961
8	11	5.2126	98.03	1.355	80.78	18.8	92.57	6.521
8	12	5.2235	98.05	1.335	81.29	18.28	92.66	6.393
8	13	5.2344	98.06	1.32	81.88	17.68	92.66	6.36
8	14	5.2455	98.06	1.31	82.5	17.04	92.77	6.26
9	7	5.2404	98.06	1.314	82.19	17.36	92.7	6.321
9	8	5.2509	98.06	1.31	82.77	16.77	92.84	6.198
9	9	5.2615	98.04	1.321	83.37	16.16	93	6.055
9	10	5.2723	98.01	1.345	83.96	15.56	93.12	5.943
9	11	5.2831	97.97	1.377	84.63	14.88	93.22	5.826
9	12	5.2942	97.94	1.395	85.31	14.19	93.33	5.691
9	13	5.3053	97.92	1.399	85.98	13.5	93.46	5.537
9	14	5.3166	97.9	1.409	86.72	12.75	93.63	5.377
10	7	5.3119	97.91	1.403	86.41	13.06	93.56	5.44
10	8	5.3225	97.88	1.423	87.1	12.37	93.72	5.311
10	9	5.3333	97.85	1.454	87.73	11.72	93.87	5.215
10	10	5.3443	97.81	1.486	88.43	11.01	94.01	5.104
10	11	5.3554	97.8	1.498	89.13	10.31	94.11	4.963
10	12	5.3666	97.8	1.494	89.88	9.559	94.21	4.796
10	13	5.378	97.8	1.49	90.54	8.901	94.31	4.667
10	14	5.3895	97.79	1.494	91.16	8.275	94.44	4.577
11	7	5.3851	97.8	1.492	90.94	8.5	94.4	4.606
11	8	5.3959	97.79	1.497	91.54	7.891	94.53	4.531
11	9	5.4069	97.78	1.5	92.12	7.303	94.64	4.458
11	10	5.4181	97.77	1.496	92.68	6.732	94.71	4.376
11	11	5.4294	97.77	1.485	93.22	6.183	94.77	4.291
11	12	5.4408	97.77	1.468	93.76	5.615	94.83	4.207
11	13	5.4524	97.78	1.444	94.22	5.127	94.89	4.141
11	14	5.4641	97.8	1.406	94.68	4.637	94.92	4.086
12	7	5.4601	97.79	1.42	94.53	4.795	94.92	4.102
12	8	5.4711	97.83	1.377	94.93	4.374	94.92	4.061
12	9	5.4823	97.87	1.329	95.29	4.001	94.89	4.036
12	10	5.4937	97.9	1.287	95.62	3.663	94.85	4.03
12	11	5.5052	97.92	1.266	95.85	3.419	94.82	4.048
12	12	5.5169	97.93	1.241	96.06	3.207	94.81	4.098
12	13	5.5287	97.98	1.192	96.24	3.026	94.81	4.188
12	14	5.5406	98.04	1.123	96.38	2.879	94.79	4.307
13	7	5.537	98.02	1.146	96.34	2.922	94.8	4.266
13	8	5.5482	98.07	1.089	96.43	2.824	94.75	4.376
13	9	5.5596	98.09	1.064	96.44	2.801	94.65	4.476
13	10	5.5712	98.07	1.072	96.37	2.854	94.5	4.552
13	11	5.5829	98.06	1.074	96.26	2.945	94.33	4.65

V→V-1 V	J-1→J J	Wave-length	M92		M98		M99	
			T%	R%	T%	R%	T%	R%
13	12	5.5948	98.09	1.03	96.16	3.033	94.21	4.795
13	13	5.6068	98.14	0.9616	96.04	3.141	94.11	4.974
13	14	5.619	98.17	0.9132	95.86	3.317	93.98	5.16
14	7	5.6158	98.17	0.9211	95.92	3.264	94.01	5.115
14	8	5.6272	98.18	0.9054	95.69	3.487	93.86	5.276
14	9	5.6389	98.16	0.9138	95.37	3.796	93.68	5.438
14	10	5.6507	98.15	0.9196	95.03	4.132	93.5	5.584
14	11	5.6626	98.16	0.9076	94.69	4.472	93.36	5.719
14	12	5.6747	98.17	0.8927	94.33	4.828	93.25	5.846
14	13	5.687	98.16	0.8925	93.94	5.215	93.17	5.972
14	14	5.6994	98.14	0.9118	93.52	5.63	93.1	6.092
15	7	5.6966	98.14	0.9075	93.59	5.56	93.11	6.073
15	8	5.7083	98.11	0.9356	93.19	5.948	93.05	6.173
15	9	5.7201	98.06	0.9747	92.78	6.364	92.99	6.259
15	10	5.7321	98.01	1.015	92.37	6.775	92.92	6.31
15	11	5.7443	97.97	1.047	91.95	7.197	92.85	6.313
15	12	5.7567	97.95	1.067	91.47	7.682	92.78	6.258
15	13	5.7692	97.92	1.087	91.01	8.143	92.75	6.188
15	14	5.7818	97.87	1.137	90.53	8.633	92.79	6.145
16	7	5.7795	97.89	1.122	90.64	8.522	92.77	6.149
16	8	5.7914	97.81	1.194	90.21	8.956	92.88	6.143
16	9	5.8035	97.72	1.28	89.82	9.361	93.04	6.127
16	10	5.8157	97.64	1.359	89.42	9.76	93.2	6.012
16	11	5.8281	97.57	1.409	89.07	10.1	93.33	5.796
16	12	5.8407	97.5	1.462	88.69	10.45	93.48	5.526
16	13	5.8535	97.4	1.534	88.31	10.8	93.68	5.328
16	14	5.8664	97.26	1.632	87.89	11.17	93.93	5.168
17	7	5.8645	97.27	1.624	87.92	11.14	93.91	5.18
17	8	5.8767	97.14	1.703	87.55	11.46	94.1	5.014
17	9	5.889	97.04	1.744	87.24	11.7	94.19	4.768
17	10	5.9015	96.96	1.763	86.98	11.89	94.19	4.45
17	11	5.9142	96.85	1.802	86.71	12.08	94.18	4.08
17	12	5.927	96.68	1.898	86.43	12.28	94.23	3.737
17	13	5.94	96.49	2.019	86.16	12.49	94.35	3.428
17	14	5.9532	96.34	2.112	85.92	12.69	94.51	3.139
18	7	5.9518	96.35	2.107	85.94	12.68	94.5	3.161
18	8	5.9642	96.27	2.145	85.76	12.84	94.66	2.903
18	9	5.9768	96.23	2.147	85.64	12.95	94.9	2.628
18	10	5.9895	96.21	2.138	85.6	12.99	95.21	2.35
18	11	6.0024	96.18	2.142	85.62	12.97	95.57	2.092
18	12	6.0155	96.1	2.183	85.65	12.92	95.97	1.818
18	13	6.0288	95.96	2.273	85.63	12.9	96.24	1.612
18	14	6.0422	95.75	2.405	85.55	12.91	96.35	1.456

V→V-1 V	J-1→J J	Wave-length	M92		M98		M99	
			T%	R%	T%	R%	T%	R%
19	7	6.0414	95.77	2.394	85.56	12.91	96.35	1.467
19	8	6.0541	95.54	2.533	85.48	12.91	96.33	1.336
19	9	6.0669	95.32	2.646	85.45	12.84	96.16	1.211
19	10	6.0799	95.13	2.724	85.48	12.7	95.89	1.091
19	11	6.0931	94.96	2.772	85.56	12.51	95.58	0.9883
19	12	6.1064	94.83	2.801	85.71	12.28	95.29	0.918
19	13	6.12	94.72	2.818	85.9	12.01	95.03	0.8952
19	14	6.1337	94.65	2.831	86.12	11.75	94.85	0.9452
20	7	6.1335	94.65	2.83	86.11	11.76	94.86	0.9388
20	8	6.1464	94.61	2.84	86.32	11.54	94.77	1.055
20	9	6.1595	94.6	2.833	86.56	11.31	94.71	1.234
20	10	6.1727	94.68	2.779	86.87	11.04	94.65	1.476
20	11	6.1862	94.82	2.674	87.2	10.75	94.56	1.728
20	12	6.1998	95.02	2.529	87.59	10.41	94.45	1.998
20	13	6.2136	95.23	2.384	87.97	10.08	94.33	2.231
20	14	6.2277	95.39	2.272	88.31	9.796	94.22	2.392
21	7	6.228	95.39	2.272	88.31	9.796	94.22	2.392
21	8	6.2412	95.47	2.229	88.56	9.59	94.15	2.448
21	9	6.2546	95.43	2.279	88.71	9.462	94.12	2.375